

MOMENTUM EXCHANGE IN COAXIAL JET FLOWS

**A THESIS SUBMITTED TO
THE GRADUATE SCHOOL OF NATURAL AND APPLIED SCIENCES
OF
MIDDLE EAST TECHNICAL UNIVERSITY**

BY

EKİM ATILLA PEKER

**IN PARTIAL FULFILLMENT OF THE REQUIREMENTS
FOR
THE DEGREE OF MASTER OF SCIENCE
IN
CIVIL ENGINEERING**

DECEMBER 2005

Approval of the Graduate School of Natural and Applied Sciences

Prof. Dr. Canan Özgen
Director

I certify that this thesis satisfies all the requirements as a thesis for the degree of Master of Science.

Prof. Dr. Erdal Çokça
Head of Department

This is to certify that we have read this thesis and that in our opinion it is fully adequate, in scope and quality, as a thesis for the degree of Master of Science.

Assoc. Prof. Dr. İsmail Aydın
Supervisor

Examining Committee Members

Prof. Dr. Mustafa Göğüş (METU, CE) _____

Assoc. Prof. Dr. İsmail Aydın (METU, CE) _____

Asst. Prof. Dr. Burcu Altan Sakarya (METU, CE) _____

Dr. Mehmet Ali Kökpınar (METU, CE) _____

MSc. Emre Öztürk (ANOVA LTD.) _____

I hereby declare that all information in this document has been obtained and presented in accordance with academic rules and ethical conduct. I also declare that, as required by these rules and conduct, I have fully cited and referenced all material and results that are not original to this work.

Name, Last name: Ekim Atilla PEKER

Signature:

ABSTRACT

MOMENTUM EXCHANGE IN COAXIAL JET FLOWS

Peker, Ekim Atilla

M.S., Department of Civil Engineering

Supervisor : Assoc. Prof. Dr. İsmail Aydın

December 2005, 56 pages

Coaxial jet flows have a considerable practical application area as water jet pumps. Efficiency of such systems is affected by complex turbulence mechanisms and large-scale vortex structures formed in the mixing regions. An experimental setup is constructed to estimate the momentum exchange rates and mixing of the two jet flows from the coaxial pipes. Pressure distributions along the mixing pipe wall are measured for different flow ratios of the jets. In addition to present experiments, numerical data of two experimental studies from the literature are considered as test cases. Numerical solutions for the test cases are obtained using FLUENT. Experimental and numerical results are compared and adequacy of FLUENT solution is illustrated.

Keywords: confined coaxial jets, momentum exchange, jet pump

ÖZ

EŞ EKSENLİ JET AKIMLARINDA MOMENTUM DEĞİŞİMİ

Peker, Ekim Atilla

Yüksek Lisans, İnşaat Mühendisliği Bölümü

Tez Yöneticisi : Doç. Dr. İsmail Aydın

Aralık 2005, 56 sayfa

Eş eksenli jet akımları su pompası olarak oldukça geniş bir pratik uygulama alanına sahiptir. Bu tür sistemlerin verimliliği kompleks türbülans mekanizma ve geniş ölçek vorteks yapılardan etkilenmektedir. Eş eksenli borulardan çıkan jet akımının momentum değişim oranını ve karışımını tahmin edebilmek için bir deney düzeneği kurulmuştur. Jetlerin farklı debi oranları için karışım borusu duvarı boyunca basınç dağılımı ölçülmüştür. Güncel deneye ilave olarak, literatürdeki iki adet deneyin numerik verileri deney durumu olarak alınmıştır. FLUENT kullanılarak, deney durumları için numerik çözümler sağlanmıştır. Deneysel ve sayısal çözümler karşılaştırıp FLUENT'in yeterliliği gösterilmiştir.

Anahtar kelimeler: Sınırlandırılmış eşeksenli jetler, momentum değişimi, jet pompası.

ACKNOWLEDGMENTS

The research presented in this thesis has been made possible with contributions from many individuals to whom I am indebted. This study was performed under the supervision of Dr. İsmail Aydın. I would like to express my sincere appreciation for his invaluable support, guidance and insights throughout my study.

I would like to thank Emre Öztürk for his support while solving numerical model in FLUENT and answering all my related questions with great patience.

I would like to thank my employers Mr. Roberto Rossetti and Mr. Hasan Ali Adıgüzel for their understanding, support and providing me additional permission to finish my thesis.

I would like to thank to my family, for their love, support and understanding during my life. I am greatly indebted to them for everything that they have done for me.

TABLE OF CONTENTS

	PAGE
PLAGIARISM.....	iii
ABSTARCT.....	iv
ÖZ	v
ACKNOWLEDGMENTS.....	iv
TABLE OF CONTENTS.....	vii
CHAPTER	
1. INTRODUCTION.....	1
1.1. INTRODUCTION.....	1
1.2. LITERATURE SURVEY.....	3
1.3. SCOPE OF THE STUDY	6
2. EXPERIMENTAL STUDIES.....	7
2.1. CASE A: EXPERIMENTS OF THIS STUDY	7
2.1.1. Experimental Setup	7
2.1.2. Methodology	12
2.1.3. Evaluation of Experimental Data	13
2.1.3.1. Discharge and Velocity of the Primary Stream.....	13
2.1.3.2. Estimation of Secondary Stream Discharge.....	14
2.1.3.3. Pressure Distribution.....	16
2.1.3.4. Measured Velocity Profiles at the end of Mixing Region	17
2.2. PREVIOUS EXPERIMENTAL STUDIES.....	18
2.2.1. Case-B: Experimental Study of RazinskY AND Brighton (1971)	18
2.2.2. Case C: Experimental Study of Shimizu, Nakamura, Kuzuhara, and Kutara (1987)	20

	PAGE
3. COMPUTATIONAL ANALYSIS.....	23
3.1. FEATURES OF FLUENT.....	23
3.2. NUMERICAL MODEL FOR CASE - A.....	24
3.2. NUMERICAL MODEL FOR CASE B.....	26
3.3. NUMERICAL MODEL FOR CASE C.....	27
4. RESULTS AND DISCUSSIONS.....	30
4.1. RESULTS AND DISCUSSIONS FOR CASE A.....	30
4.1.1. Discharges and Average Velocities.....	30
4.1.2. Craya Curtet Number and Initial Conditions.....	32
4.1.3. Dimensionless Velocity Profiles.....	33
4.1.4. Experimental and Numerical Pressure Variation.....	38
4.2. RESULTS AND DISCUSSIONS FOR CASE B.....	44
4.3. RESULTS AND DISCUSSIONS FOR CASE C.....	47
4.3. SEPERATION BUBBLES AND ENERGY DISSIPATION.....	50
5. CONCLUSIONS.....	53
REFERENCES.....	55

CHAPTER 1

INTRODUCTION

1.1. INTRODUCTION

The study intends to investigate momentum exchange of the jets expanding inside a pipe. A large portion of the study is devoted to the jets taking place inside a constant diameter pipe. Some studies related with the expansion of the jet inside a variable diameter pipe are also presented.

According to position of the driving jet, there are two types of confined coaxial jets which are named as central and annular jets shown in Fig 1.1.

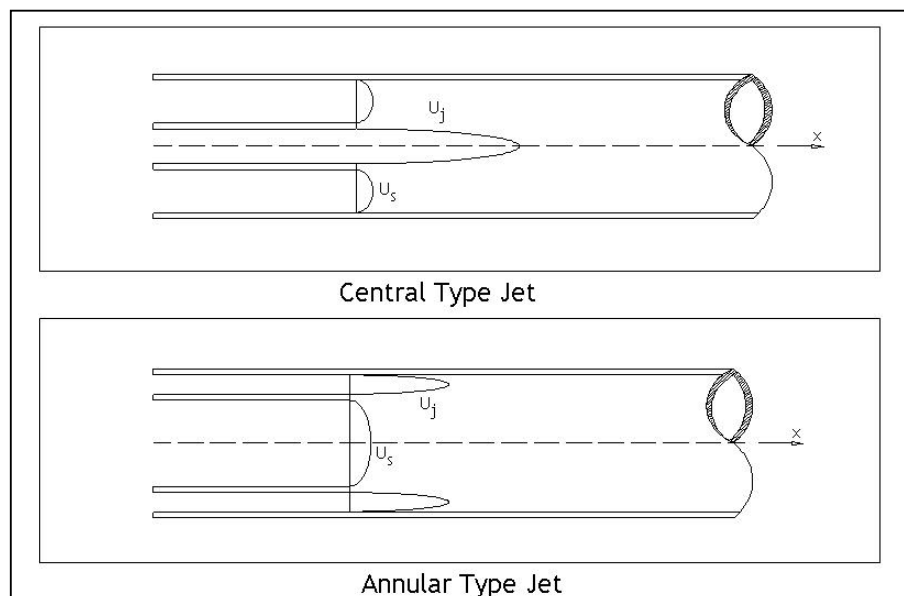


Figure 1.1: Central Jet and Annular Jets

In the central type, a circular jet flow is issuing axially inside a pipe and surrounding fluid moves in the same direction. In general the jet and surrounding flows are called as primary and secondary stream. The flow inside the mixing pipe is given in Figure 1.2.

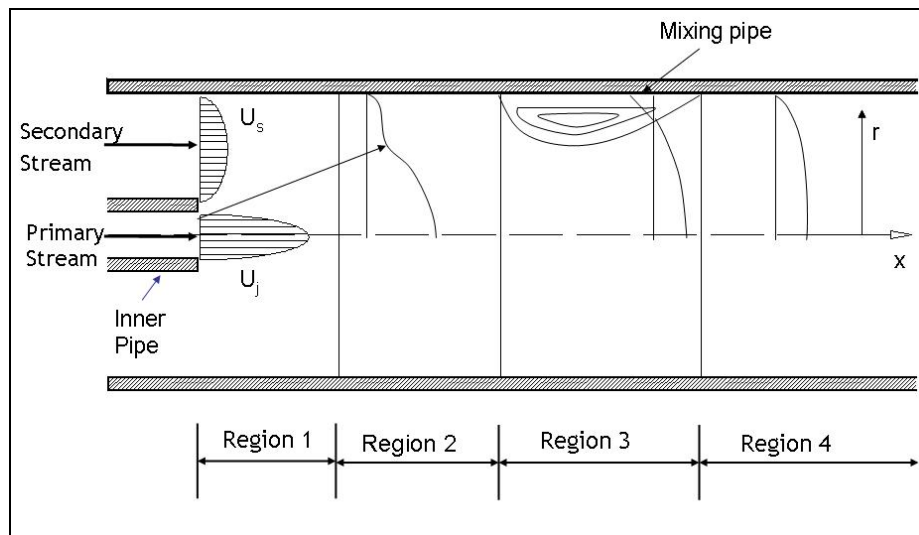


Figure 1.2: Flow inside coaxial flow adapted from Rajatman (1976)

Considering the flow properties, the coaxial confined jet can be divided into four regions. In Region 1, primary stream issues as a jet and entrains with secondary stream. Two different boundary layer and shear regions develop. In Region 2 the jet grows in diameter along the shear layer and meanwhile secondary stream consumes. In some flow cases, recirculation takes place if the secondary flow is consumed and fully entrained before the jet expands and reaches to walls. At the end of Region 3, the mixing will be completed and the flow will be uniform recovered uniform flow characteristics.

The confined jet is more complicated from other free jet problems since the confining walls cause pressure gradient which effects the rate of spread of the jet, rate of growth of boundary layer and velocity profile shape.

The annular type jet is different than central type in terms of the location of the jet. In this case the surrounding flow is issuing as a jet and the circular center flow is considered as a suction flow.

Both configurations have practical usages and serve as a jet pump. If jet is located at the center, the pump is called as center type jet pump and if the surrounding fluid serves as a jet then the pump is called as annular jet pump. Transferring the high velocity of jet to one of lower velocity, the jet pump performs. High pressure in the jet line is converted into high kinetic energy by decreasing the jet diameter of the jet nozzle. The reduction of pressure will provide suction for secondary fluid and by means of high velocity transferred two streams will be mixed. Thus the particles of secondary fluid will be accelerated by the impact of high kinetic energy provided by jet. Generally a jet pump is suited with a diffuser and high kinetic energy is converted into potential energy. Then mixing event will be totally completed and flow will be uniform.

1.2. LITERATURE SURVEY

Experimental and numerical investigations of confined coaxial jet have been reported detailed in the literature.

Rajataman (1976) gathered all the information and presented a detailed treatment of flow characteristics of turbulent jets in a book called as “Turbulent Jets” which was published in 1976. His studies present the typical experimental results, which are related with the similarity of the mean square of the velocity

fluctuations and turbulence shear stress profiles in accordance with the idea of presented experiments.

Study of Razinsky and Brighton (1971) is a complete investigation of the measurements of wall static pressure, mean velocity, turbulence and Reynolds stress throughout the flow field for different velocity and diameter ratios.

Khodadadi and Vlachos (1989) studied the turbulent mixing of a primary jet and its surrounding fluids in a constant diameter pipe with various inlet connections that result in flow separation. A numerical model was developed using a two-equation turbulence model in conjunction with a finite difference based numerical prediction procedure. The numerical model was tested for selected experimental results from literature.

Choi, Gessner and Oates (1986) investigated the mixing of a subsonic air jet with a coaxial secondary stream experimentally. The effects of adverse pressure gradient on mixing characteristics in the initial region and transition region was observed. In the study it was concluded that the mixing and spreading of the shear layer increase due to presence of an adverse pressure gradient.

Elger, Taylor, Liou (1994) performed experiments using air annular type circular jet in a constant diameter pipe. Executing a dimensionless analysis for an annular jet, it is stated that recirculation correlates with a dimensionless parameter, J , which is the ratio of momentum of jet to the total momentum of jet and secondary flows. It is concluded that recirculation depends mostly on momentum ratio and less on area ratio and no dependence on Reynolds number.

In addition to the studies of confined coaxial jets there are also numerous investigations related with the practical application of confined coaxial jets.

Mueller (1964) observed the performance and efficiency of central jet type experimentally. Considering the head losses occurring in the system, the efficiency of the jet pump was formulated. The affects of different geometric parameters such as location of driving nozzle, area ratio, length of the chamber, and diffuser angle were investigated.

Reddy and Kar (1968) followed the same approach which was described in Mueller's study is followed in order to find the head losses of each parts and to formulate efficiency of the pump. Besides the observation for the effect of geometric configuration on the efficiency, two different materials were used in the design of the pump and the effects on the head losses and as well as efficiency is described.

Sanger (1970) evaluated several low area pumps experimentally, investigating the affects of the principal geometrical variables such as area ratio, throat length, and nozzle spacing in efficiency and pressure distribution.. In the study a commercial type jet nozzle was used. The study is also intended to define the efficiency under non-cavity and cavity flow conditions.

Study of Shimizu, Nakamura, Kuzuhara, S.Kutara (1987) investigated the optimum design conditions of annular jet pumps. 25 different geometrical configurations were tested. The results were compared with other studies carried out for the central jet type pumps. In addition to the studies of efficiency, the pressure distributions for different configuration of geometry and flow condition were measured experimentally.

Study of Elger, McLam, and Taylor (1991) investigated a new way to present jet pump efficiency. It is proposed that the previous definition of efficiency with a Head-Ratio, Flow Ratio curves have some problems. HR/FR approach forces the designer to estimate the head loss inside a jet pump and does not give

enough information about the operating point of the system. As a result the study proposes a new methodology and new set of curves to eliminate the problems while representing the jet pump efficiency.

1.3. SCOPE OF THE STUDY

There are two purposes of this study. First purpose is to perform experiments in order to investigate the pressure distribution and momentum exchange in confined coaxial jet flows. Second purpose is to obtain numerical solutions to confined coaxial jets using the commercial code FLUENT.

In Chapter 2, experimental setup used in the present study will be described. The evaluation of each experimental data is presented. In addition, some selected previous experiments from literature will be introduced. The setup used in that studies and initial conditions are defined.

In Chapter 3, various parameters of the numerical solver will be introduced. Then explaining the solution domain, grid generation and boundary conditions, the computational models of present and previous experimental studies are described.

The experimental data of this study and other previous experimental studies are compared with predictions obtained from numerical solutions. The results and related discussions are given in Chapter 4.

CHAPTER 2

EXPERIMENTAL STUDIES

2.1. CASE A: EXPERIMENTS OF THIS STUDY

The present experimental study is used to investigate the properties of the confined coaxial flow and to provide data in order to test the performance of the numerical solver. In this chapter, geometrical elements are introduced, methods followed during the experiment are described and basic equations used in data analysis are derived.

2.1.1. Experimental Setup

The geometry and the position of the pipes that are used are shown in Figure 2.1. This geometry is valid for the domain to be developed for the numerical model.

The setup is composed of two pipes. A relatively small diameter jet pipe is inserted inside a larger pipe. The flow inside the inner pipe, which is known as primary stream, is issuing as a jet into a constant radius mixing pipe, which is denoted by R . The inner radius and the thickness of the inner pipe are denoted as R_1 , and e , respectively. The clearance between inner pipe and mixing pipe is represented as, w . The flow between inner pipe and mixing pipe is called as secondary stream, which has a smaller velocity magnitude than the jet flow in the inner pipe. In the literature, considering the flow properties of confined jet, the secondary stream is also known as suction flow.

Geometrical dimensions of the coaxial system shown Figure 2.1 are given in Table 2.1.

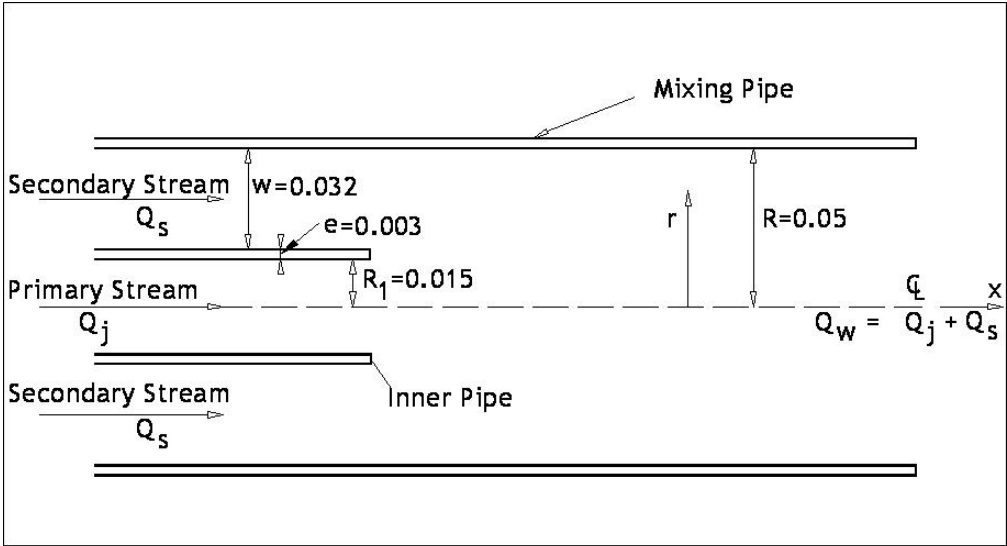


Figure 2.1: Geometry of the pipes used in the experimental study

Table 2.1 Geometrical properties of the pipes used in the experiments

Symbols	Definition	Value
R	Radius of the mixing pipe	0.05 m
R_1	Inner radius of the jet pipe	0.015 m
e	Thickness of the inner pipe	0.003 m
w	Clearance between inner pipe and Duct	0.032 m
A	Area of the mixing pipe	0.007854 m ²
A_j	Area of the jet (Flow area of primary stream)	0.000707 m ²
A_w	Flow area of the secondary stream	0.006836 m ²
R_1 / R	Ratio of radius	3.33
A_1 / A	Ratio of area	0.090017825

Figure 2.2 shows a schematic diagram of the setup. The setup is consisting of an U-type manometer, piezometer tubes, a total head tube and a weir.

The U-type manometer is installed on the surface of the inner pipe in order to measure the pressure gradient. From measured pressure gradient, the discharge of the primary stream is estimated.

There are 19-piezometer tubes installed along the mixing pipe in order to measure the pressure distribution. The first five of these piezometer tubes are used

to estimate the head loss of the secondary stream. Piezometer tube no. 6 is installed just at the location of mixing of two streams and the rest of the piezometer tubes enable to follow the pressure distribution along the mixing pipe.

At the far end of the mixing pipe a total head tube is placed in order to measure the total head. It is exactly located at 4.6 m. away from the jet pipe. The velocity profile is obtained from total head measurements.

The mixing pipe discharges into an open channel and there is a weir located at the end of the open channel which is used to measure the flow rate of the flow passing inside the mixing pipe. The flow rate of the secondary flow is computed from conservation of mass.

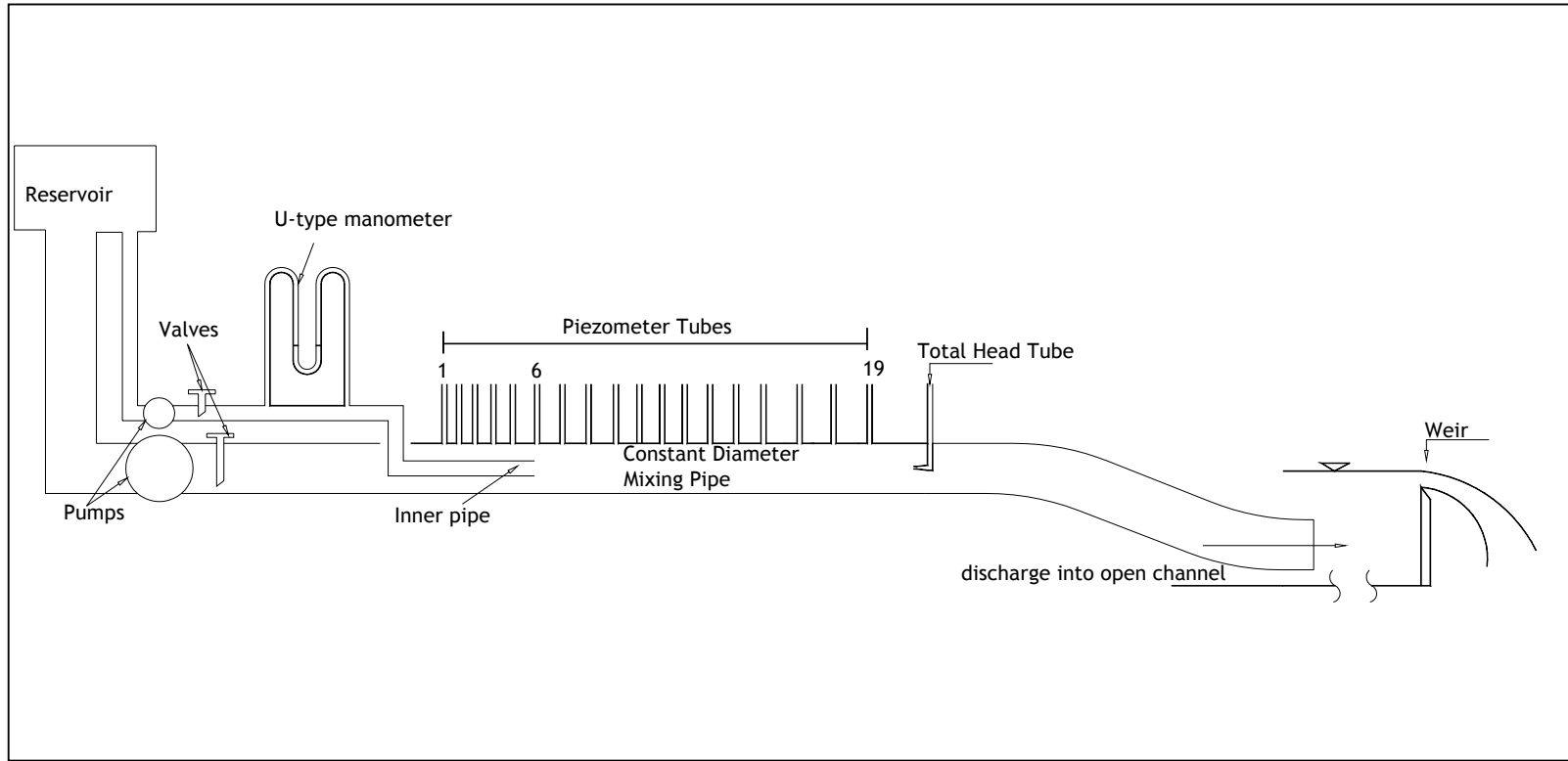


Figure 2.2: Experimental arrangement

2.1.2. Methodology

Through the experiments the methods stated below are followed.

1. Using the valve attached to the inner pipe, the discharge of the primary stream is adjusted. The pressure drop in the inner pipe is recorded. The flow condition of primary stream is kept constant.
2. Another valve is attached to adjust the flow rate of the mixing pipe. Using this valve, the flow rate of secondary stream is adjusted.
3. After setting primary and secondary stream discharges, the head of weir in the open channel is recorded in order to determine the total flow rate of mixing pipe.
4. The pressure head along the mixing pipe are recorded using piezometer tubes.
5. Finally, using the total head tube located at the far end of the pipe, total head values are recorded. As a result one case of the experiment is completed.
6. The flow condition of primary stream is kept constant and the flow condition of the secondary stream is changed. For this new case of experiment, data are collected, following the above stated order.
7. Under the same flow condition of the primary stream, changing the flow condition of the secondary stream experimental data are collected. Then the flow in the primary stream is changed using the attached valve. The pressure drop of new flow condition is recorded from U-type manometer. In the experiments three different flow rates of the primary stream are used.

2.1.3. Evaluation of Experimental Data

2.1.3.1. Discharge and Velocity of the Primary Stream

U-type manometer is installed in order to measure the pressure drop in the primary pipe and this is given schematically in Figure 2.3

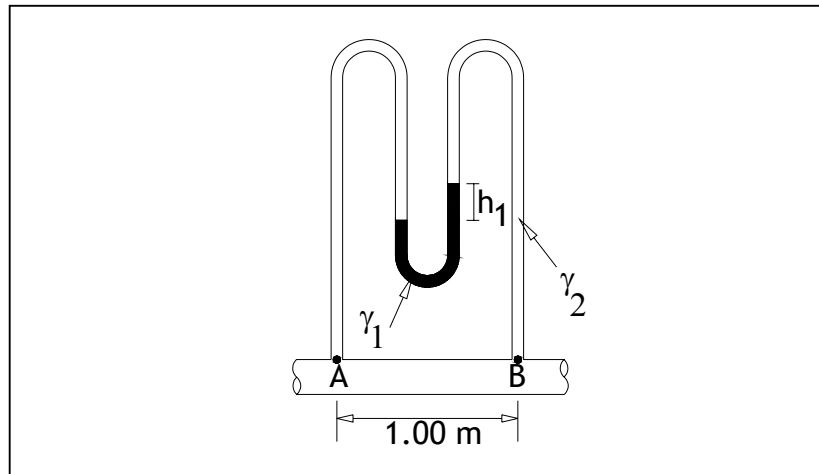


Figure 2.3: U-type manometer

Pressure drop, ΔP , is measured from the U-type manometer is computed from the following equation

$$\Delta P = h_1(\gamma_1 - \gamma_2) \quad [2.1]$$

where h_1 is the deflection in the U-type manometer, γ_1 is the specific weight of mercury and γ_2 is the specific weight of water

Using the measured head loss, discharges in the primary stream are computed from the Darcy-Weisbach equation.

FLUENT is used to solve the uniform pipe flow problem for a given average velocity, utilizing the $k-\epsilon$ turbulence model. The velocity profile obtained from uniform pipe flow solution is used as the inflow boundary condition at the inlet section of the setup.

2.1.3.2. Estimation of Secondary Stream Discharge

There is a sharp-crested weir placed at the end of the experimental setup so that total discharge of primary and secondary streams is measured from this weir. The weir discharge is computed from the measured head over the weir. The adopted equation for sharp crested weir is given as follows.

$$Q_w = C_d \frac{2}{3} \sqrt{2gb} H^{3/2} \quad [2.2]$$

where

$$C_d = 0.611 + 0.075 \left(\frac{H}{W} \right).$$

W is the weir height, b is the weir width, and g is the gravitational acceleration.

Considering the conservation of mass, flow rate of the secondary stream is computed from

$$Q_s = Q_w - Q_j \quad [2.3]$$

The primary stream discharge, total weir discharge and the corresponding secondary flow discharge for each experimental case are given in Table 2.2

Table 2.2: Primary stream, secondary stream and weir discharges and average velocities

Cases		primary stream		secondary stream		Weir	
	$\frac{\Delta P}{\Delta X}$	Q_j	V_j	Q_s	V_s	Q_w	V_w
	kN/m ² /m	m ³ /s	m/s	m ³ /s	m/s	m ³ /s	m/s
A-1	12.979	0.0036	5.060	0.0069	1.0106	0.01049	1.335
A-2	12.979	0.0036	5.060	0.0047	0.6915	0.0083	1.057
A-3	12.979	0.0036	5.060	0.0044	0.6431	0.0080	1.015
A-4	12.979	0.0036	5.060	0.0032	0.4633	0.0067	0.859
A-5	12.979	0.0036	5.060	0.0026	0.3795	0.0062	0.786
A-6	12.979	0.0036	5.060	0.0022	0.3193	0.0058	0.733
A-7	12.979	0.0036	5.060	0.0012	0.1786	0.0048	0.611
A-8	12.979	0.0036	5.060	0.0005	0.0708	0.0041	0.517
A-9	11.248	0.0033	4.680	0.0059	0.8634	0.0092	1.173
A-10	11.248	0.0033	4.680	0.0035	0.5113	0.0068	0.866
A-11	11.248	0.0033	4.680	0.0013	0.1973	0.0047	0.593
A-12	11.248	0.0033	4.680	0.0005	0.0671	0.0038	0.480
A-13	11.248	0.0033	4.680	0.0004	0.0532	0.0037	0.468
A-14	6.489	0.0025	3.488	0.0034	0.4971	0.0059	0.747
A-15	6.489	0.0025	3.488	0.0024	0.3470	0.0048	0.616
A-16	6.489	0.0025	3.488	0.0019	0.2767	0.0044	0.555
A-17	6.489	0.0025	3.488	0.0017	0.2448	0.0041	0.527
A-18	6.489	0.0025	3.488	0.0012	0.1720	0.0036	0.464

2.1.3.3. Pressure Distribution

Arrangement of piezometer tubes along the mixing pipe is shown in Figure 2.4.

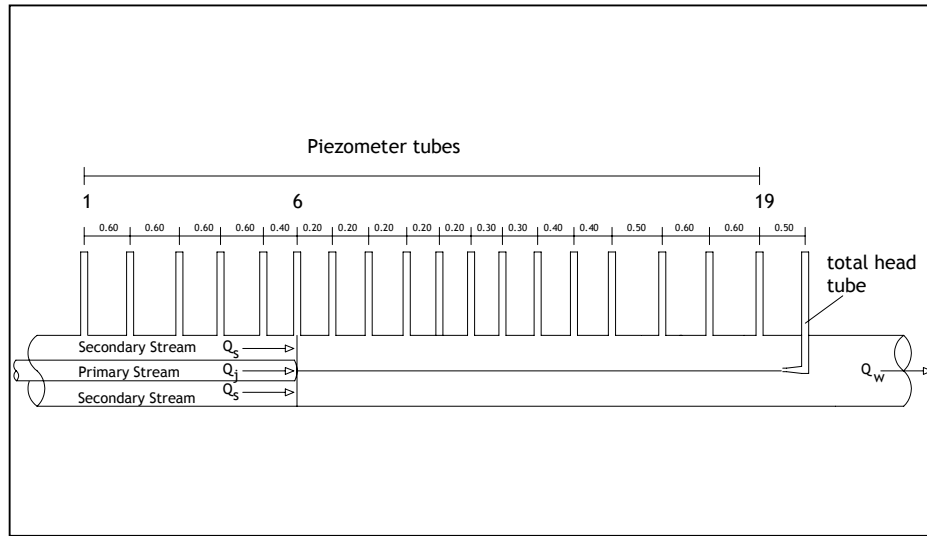


Figure 2.4: Position of piezometers

Pressure tube no.6 is exactly located at the exit of the primary stream so that it measures the pressure at the beginning of the mixing region. Pressure is given relative to entrance pressure and it is non-dimensionalized by the dynamic head of the total discharge. The dimensionless pressure is defined as:

$$C_p = \frac{p_i - p_6}{\frac{1}{2} \rho U_w^2} \quad [2.4]$$

where

C_p : Dimensionless pressure

P_i : Wall pressure at the station i (N/m^2)

P_6 : Reference wall pressure at the entrance (N/m^2)

ρ : Density of fluid (kg/m^3)

U_w : Average velocity (m/s)

2.1.3.4. Measured Velocity Profiles at the end of Mixing Region

The total head tube is installed at far end of the mixing pipe. Point velocity is measured by traversing the total head tube along the pipe radius. Piezometer head at the location of total head tube is interpolated from recorded piezometric line. The velocity head measurement is given schematically in Figure 2.5

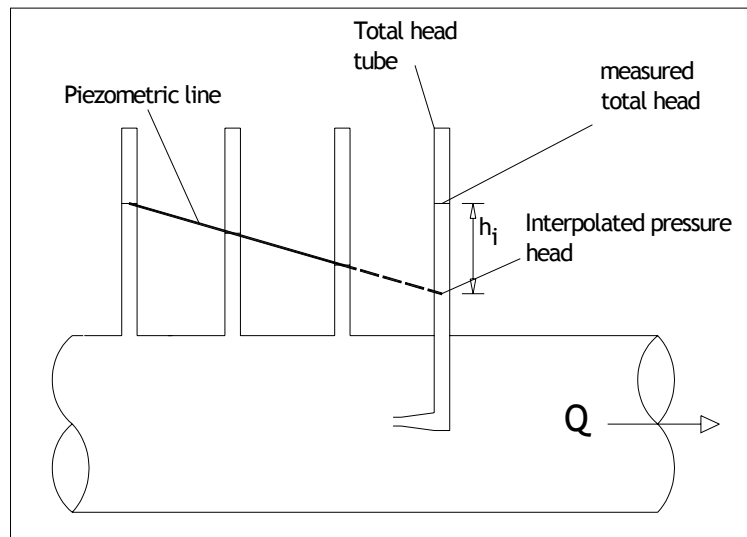


Figure 2.5: Velocity measurements

Point velocity is computed from

$$u_i = \sqrt{2gh_i} \quad [2.5]$$

where h_i is the measured velocity head.

The measured and computed velocity profiles are compared in Chapter 4

2.2. PREVIOUS EXPERIMENTAL STUDIES

As it is stated before, one of the aims of the study is to test the performance of the numerical solver by comparing with the results selected from literature. The studies of Razinsky and Brighton (1971) and study of Shimizu, Nakamura, Kuzuhara, Kutara (1987) are considered as additional test cases. In this section, experimental setups used in these studies and the initial flow conditions of primary and secondary streams are introduced.

2.2.1. Case-B: Experimental Study of Razinsky AND Brighton (1971)

The experimental study of Razinsky and Brighton were carried out in a constant cross section mixing pipe. Their experimental setup is illustrated in Figure 2.6.

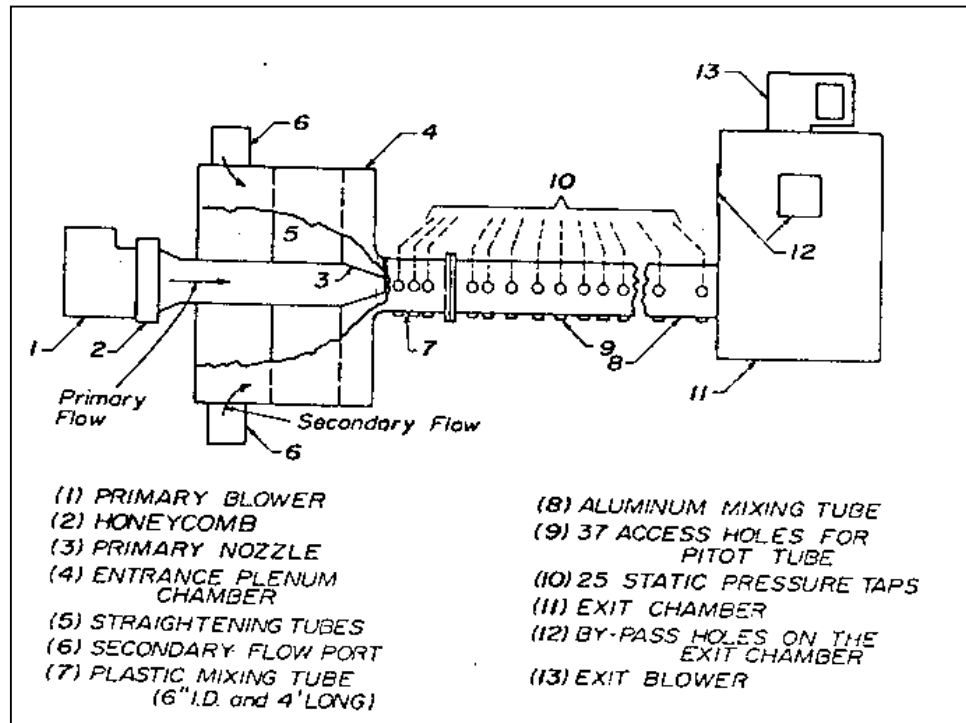


Figure 2.6: Setup used in experimental study of Razinsky and Brighton (1971)

In this study a very detailed pressure, mean velocity and turbulence properties of confined coaxial jet flow are examined but, our main interest is in pressure variation and mean velocity so that they can be compared with numerical solutions.

The radius ratio $R_1 / R = 1/3$ and the velocity ratio, $U_j / U_s = 5$ and 9 are included as the test cases.

2.2.2. Case C: Experimental Study of Shimizu, Nakamura, Kuzuhara, and Kutara (1987)

In this study, the surrounding flow is issuing as a jet and central flow is considered as a suction flow. In the study, 25 geometric arrangements were tested in order to explain the efficiency of the pump. Since the exact location where the head differences are recorded and order of friction losses through the pipe cannot be understood in a detailed manner, it is difficult to accomplish a numerical study to solve the efficiency. In addition to study of efficiency, a particular setup was constructed in order to investigate the pressure variation in the annular jets. The setup used in pressure variation analysis is given Figure 2.7.

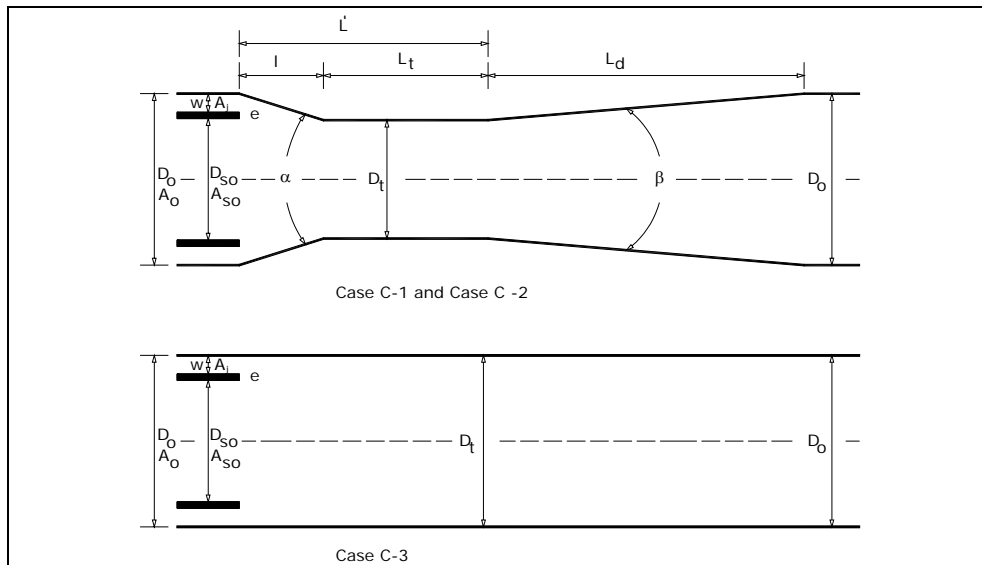


Figure 2.7: Configuration and dimension of Case C

The variables used in description of the geometry are

- D_o : Inner Diameter of the suction line
- A_o : Inner Area of the suction line
- D_{so} : Exit diameter of central nozzle
- A_{so} : Exit area of central nozzle
- w : Clearance between suction pipe and duct
- D_t : Inner diameter of mixing chamber
- A_t : Inner Area of mixing chamber
- L_t : Length of mixing chamber
- α : Reduction angle
- β : Diffuser angle
- e : Thickness of central nozzle
- L_d : Length of diffuser

In the study the jet and suction flow rate ratio is defined as M

$$M = Q_s / Q_j \quad [2.6]$$

Considering the area ratio of entrance A_{so} / A_j and geometry of the mixing pipe, the experiments were executed under three different geometrical arrangements. In Cases C-1 and C-2, the mixing pipe has the same cross section, where as the area ratio of entrance is different. For Case C-3 the mixing pipe is selected as straight in cross section. In accordance with Figure 2.7, the dimensions of the geometrical variables are given Table 2.3.

Table 2.3: Dimensions of Case C-1, C-2, C-3

Cases	C-1	C-2	C-3
D_o (m)	0.055		
A_o (m ²)	0.00238		
D_{so} (m)	0.039	0.043	0.047
A_{so} (m ²)	0.00119	0.00145	0.00173
w (m)	0.006	0.004	0.002
A_t (m ²)	0.00092	0.00064	0.00033
D_t (m)	0.0381		0.055
A_t (m ²)	0.00114		0.00238
L_t (m)	0.1553		-
l (m)	0.0537		-
L' (m)	0.209		-
L_d (m)	0.3795		-
α	18°		-
β	5.8°		-

In the study, the discharge ratios measured as initial conditions for each case are given in Table 2.4

Table 2.4: Flow ratios of each case

Case	C-1	C-2	C-3
M	0.02	0.04	0.01
	0.19	0.30	0.11
	0.34	0.58	0.19
	0.33		0.34

CHAPTER 3

COMPUTATIONAL ANALYSIS

Computational Fluid Dynamics (CFD) code FLUENT is used to obtain numerical solutions. In this chapter the methods used in will be explained considering the solution domain, boundary conditions, grid generation and turbulence model.

One of the main purposes of this study is to compute the confined coaxial problem numerically. This is accomplished by comparing the numerical results with the results of the present and previous experimental studies. Therefore, identical flow conditions and geometrical configurations are imposed in the numerical models.

3.1. FEATURES of FLUENT

Before presenting the results of numerical studies, the CFD code FLUENT is introduced briefly, so that reader of this study will be familiar with FLUENT environment. The methodology to be given here will be valid for present studies. Development of the geometry, grid generation, material specification, determination of boundary conditions, selection of solution model, and solution control methods are the main discussion items.

Using the preprocessor called as Gambit, solution domain and grid system are developed and imported in to the FLUENT environment.

Then grid check is performed. The grid check lists the minimum and maximum x and y values of the grid in the default SI units and reports other grid features that are checked. Any errors in the grid would be reported at this time.

FLUENT has a rich database in which one can find properties of various fluids. In modeling the present study water is selected as the flowing fluid

The numerical solution to the discretized equations can be pressure based or density based.

Several eddy viscosity models can be selected as turbulence model, the standard κ - ϵ model is used in the present study.

SIMPLE method is utilized in pressure-velocity coupling. At first, first order upwind is used. After achieving certain convergence, second order upwind is used.

3.2. NUMERICAL MODEL FOR CASE - A

Computational domain for Case – A is defined by considering axisymmetry along the primary jet axis. The computational domain is given in Figure 3.1.

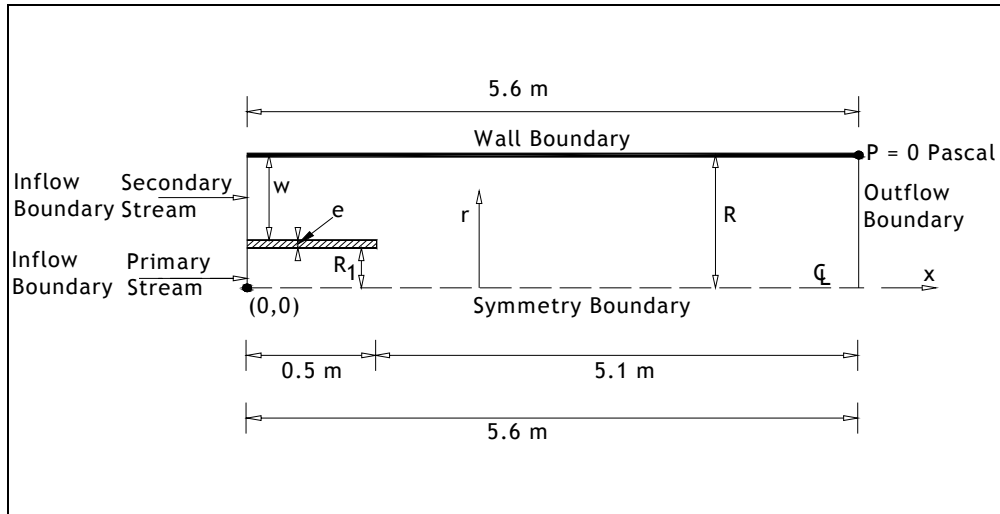


Figure 3.1: Computational domain, Case A

The domain is starting 0.5 m before the entrance of the jet so that flows in the primary and secondary streams are treated as uniform flow. The variables shown in Figure 3.1 are already given in Table 2.1.

The computational mesh is generated by Gambit. The points are clustered around the jet exit. Since the domain is so large, a part of the developed mesh at the entrance region is shown in Figure 3.2

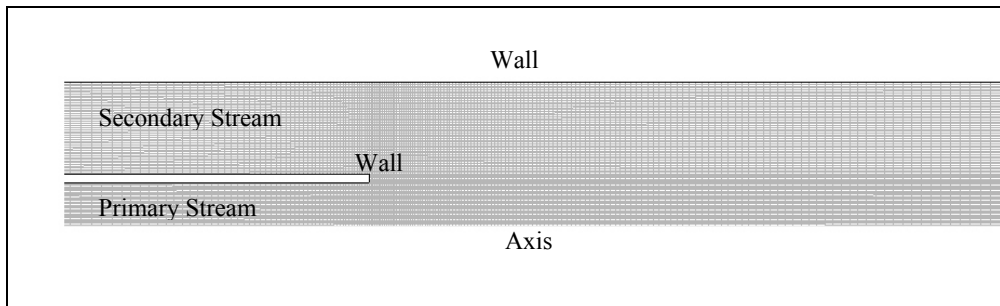


Figure 3.2: Mesh of solution domain, Case A

The primary and secondary streams are implemented as velocity inlets. Velocity profiles of two streams will be given as input and initial condition to the numerical model. The average velocity values were already presented in Table 2.2. The outflow is treated as pressure outlet and the outflow pressure is set to 0 Pascal.

3.2. NUMERICAL MODEL FOR CASE B

The computational domain used in model of the study is shown in figure 3.3. It can be noticed that the solution domain and boundary conditions are similar to Case-A.

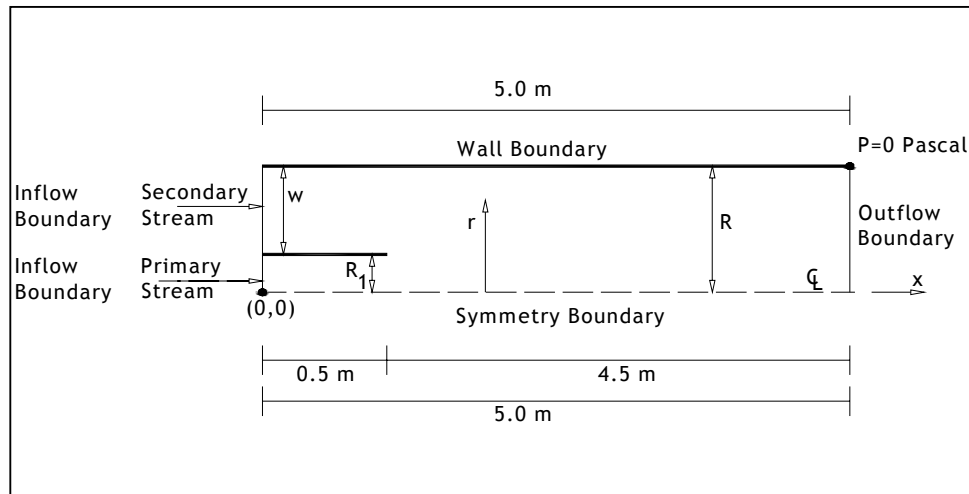


Figure 3.3: Computational domain, Case B

Here in the dimensions of the domain relevant to Figure 3.18 are as follows;

$$R = 0.03 \text{ m}$$

$$R_1 = 0.01 \text{ m}$$

$$w = 0.02 \text{ m}$$

The computational mesh is generated by Gambit. The points are clustered around the jet exit. Since the domain is so large, a part of the developed mesh at the entrance region is shown in Figure 3.4

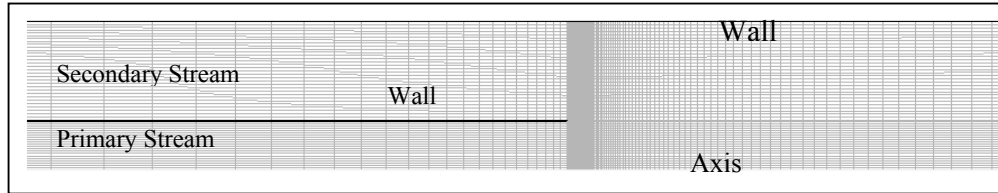


Figure 3.4: Meshing Scheme, Case B

The flowing fluid is air for this study and the properties of air is selected from material database of FLUENT.

The inflow conditions of primary and secondary stream velocities were defined in Chapter 2.

3.3. NUMERICAL MODEL FOR CASE C

This case is different from the first two cases as it has a variable cross-section of mixing pipe. In addition, the driving jet and suction jet are replaced.

The computational domain for Case C is illustrated in Figure 3.5. The basic dimensions used in experimental study were already given in Table 2.3, but in order to state the computational domain clearly, in accordance with Figure 3.5, dimensions given in that table are referred again and represented in Table 3.1.

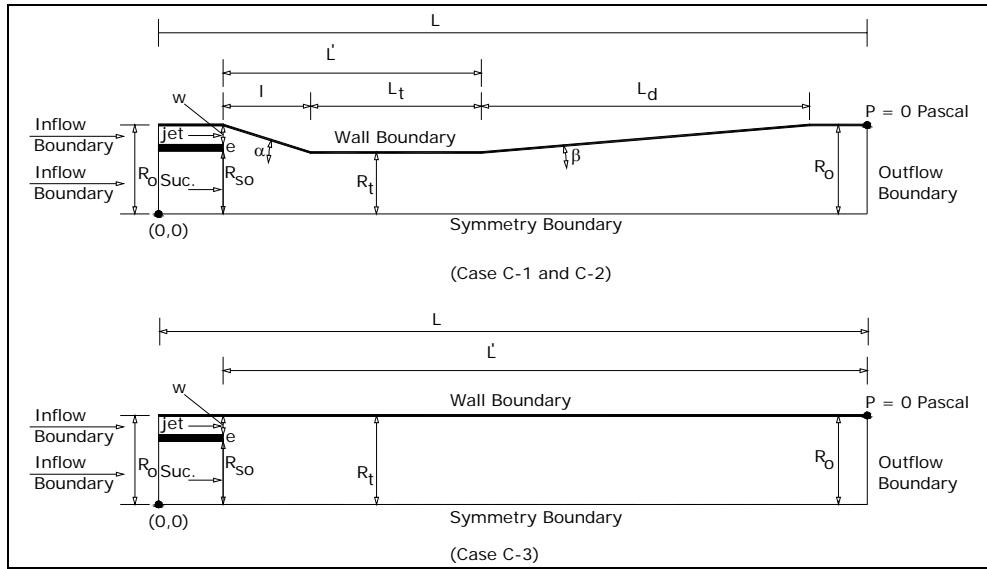


Figure 3.5 Computational domains, Case C-1, C-2, C-3

Table 3.1: Dimension of Computational Domain for Cases C -1, C-2 and C-3

Case	C -1	C - 2	C - 3
R_o (m)	0.0275		
R_{so} (m)	0.0195	0.0215	0.0275
w (m)	0.006	0.004	0.002
R_t (m)	0.019		0.0275
L_t (m)	0.1553		-
l (m)	0.0537		-
L' (m)	0.209		0.495
L_d (m)	0.3795		-
L (m)	0.594		0.535
$\alpha/2$	9°		-
$\beta/2$	2.9°		-

The meshing of the models of cases is developed in Gambit. The points are clustered around the jet exit. The developed mesh for the solution domain of Case C-1 and C-2 and C-3 are shown in Figure 3.6, and 3.7 respectively.

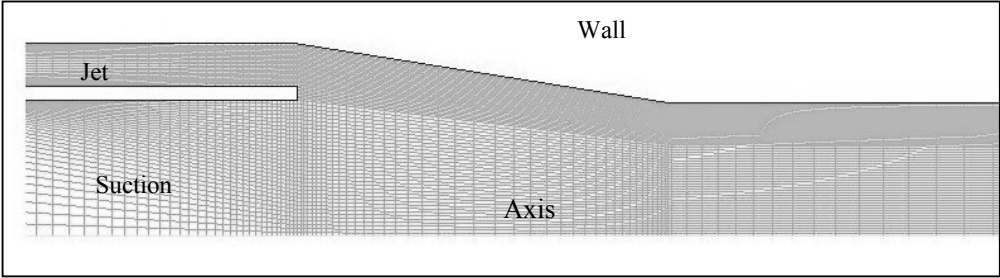


Figure 3.6 Meshing scheme for Cases C-1 and C-2

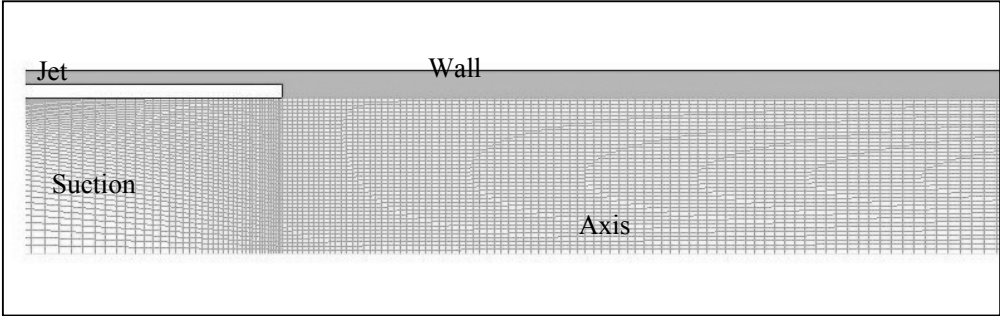


Figure 3.7: Meshing scheme for Cases C-3

The jet and suction streams are treated as velocity inlets. Average velocities of two streams are computed from imposed flow rate ratios of the study. The ratio of flow rates are already given in Table 2.4. Outflow is treated as pressure outlet and it is set to 0 Pascal.

CHAPTER 4

RESULTS AND DISCUSSIONS

4.1. RESULTS and DISCUSSIONS for CASE A

4.1.1. Discharges and Average Velocities

During the experiments, pressure drop of primary stream is measured from U-type manometer and discharge is estimated from Darcy-Weisbach equation. Total discharges in the mixing pipe are measured from weir. At the first instant discharge in the secondary stream can not be computed. Considering conservation of mass, summation of discharges of primary and secondary stream has to be equal to discharge in the pipe after mixing.

The discharges of primary and secondary stream are treated as inflow conditions for the numerical solutions. In Table 4.1, discharges and average velocities of primary and secondary streams and the flow rates in mixing pipe which are computed from experimental and numerical data are given.

Table 4.1: Discharges and velocities of primary and secondary streams and total experimental and numerical discharges and velocities of mixing pipe

Cases	primary stream		secondary stream		Weir		Computational	
	Q_j	V_j	Q_s	V_s	Q_w	V_w	Q_c	V_c
	m ³ /s	m/s	m ³ /s	m/s	m ³ /s	m/s	m ³ /s	m/s
A-1	0.0036	5.060	0.0069	1.0106	0.01049	1.335	0.0107	1.357
A-2	0.0036	5.060	0.0047	0.6915	0.0083	1.057	0.0084	1.071
A-3	0.0036	5.060	0.0044	0.6431	0.0080	1.015	0.0081	1.029
A-4	0.0036	5.060	0.0032	0.4633	0.0067	0.859	0.0069	0.873
A-5	0.0036	5.060	0.0026	0.3795	0.0062	0.786	0.0063	0.801
A-6	0.0036	5.060	0.0022	0.3193	0.0058	0.733	0.0059	0.749
A-7	0.0036	5.060	0.0012	0.1786	0.0048	0.611	0.0049	0.625
A-8	0.0036	5.060	0.0005	0.0708	0.0041	0.517	0.0042	0.530
A-9	0.0033	4.680	0.0059	0.8634	0.0092	1.173	0.0092	1.171
A-10	0.0033	4.680	0.0035	0.5113	0.0068	0.866	0.0069	0.882
A-11	0.0033	4.680	0.0013	0.1973	0.0047	0.593	0.0048	0.606
A-12	0.0033	4.680	0.0005	0.0671	0.0038	0.480	0.0039	0.492
A-13	0.0033	4.680	0.0004	0.0532	0.0037	0.468	0.0038	0.480
A-14	0.0025	3.488	0.0034	0.4971	0.0059	0.747	0.0059	0.754
A-15	0.0025	3.488	0.0024	0.3470	0.0048	0.616	0.0049	0.623
A-16	0.0025	3.488	0.0019	0.2767	0.0044	0.555	0.0044	0.561
A-17	0.0025	3.488	0.0017	0.2448	0.0041	0.527	0.0042	0.533
A-18	0.0025	3.488	0.0012	0.1720	0.0036	0.464	0.0037	0.470

4.1.2. Craya Curtet Number and Initial Conditions

The flow characteristics in the confined coaxial jet are controlled by a dimensionless number called as Craya–Curtet. In the study of J.M. Khodadadi and N. S. Vlachos (1989) Craya-Curtet number were introduced as follows:

$$Ct = \frac{U_m}{\left[(U_1^2 - U_2^2)a^2 + 0.5(U_2^2 - U_m^2) \right]^{1/2}} \quad [4.1.]$$

where

$$U_m = (U_1 - U_2) a^2 + U_2$$

U_1 : Primary stream velocity (m/s)

U_2 : Secondary stream velocity (m/s)

a : Radius ratio (R_1/R)

Using the above definition, computed C_t values and corresponding initial conditions of primary and secondary streams are summarized in Table 4.2.

Table 4.2 Craya-Curtet number for each case

Cases	U_j	U_j	U_j/U_s	C_t
	m/s	m/s		
A-1	5.060	1.011	5.006	0.990
A-2	5.060	0.691	7.317	0.770
A-3	5.060	0.643	7.868	0.738
A-4	5.060	0.463	10.921	0.622
A-5	5.060	0.379	13.334	0.569
A-6	5.060	0.319	15.847	0.532
A-7	5.060	0.179	28.332	0.447
A-8	5.060	0.071	71.471	0.384
A-9	4.680	0.863	5.421	0.935
A-10	4.680	0.511	9.153	0.679
A-11	4.680	0.197	23.716	0.468
A-12	4.680	0.067	69.742	0.385
A-13	4.680	0.053	87.927	0.376
A-14	3.488	0.497	7.017	0.789
A-15	3.488	0.347	10.053	0.647
A-16	3.488	0.277	12.607	0.583
A-17	3.488	0.245	14.250	0.554
A-18	3.488	0.172	20.280	0.490

4.1.3. Dimensionless Velocity Profiles

At the end of mixing pipe total head is recorded and velocity profile of the flow is measured accordingly. The measured velocity profile will be nondimensionalized by average velocity. The nondimensional velocity profiles are plotted against nondimensional length scale, r/R .

Similar analyses are also executed computationally in order to compare the numerical results with the experimental ones. After the numerical solution, the velocity profiles at the outflow are nondimensionalized by the average velocities

computed from numerical solution. Some selected results are shown in Figure 4.1 to 4.5 for cases A-2, 6, 8, 11 and 15.

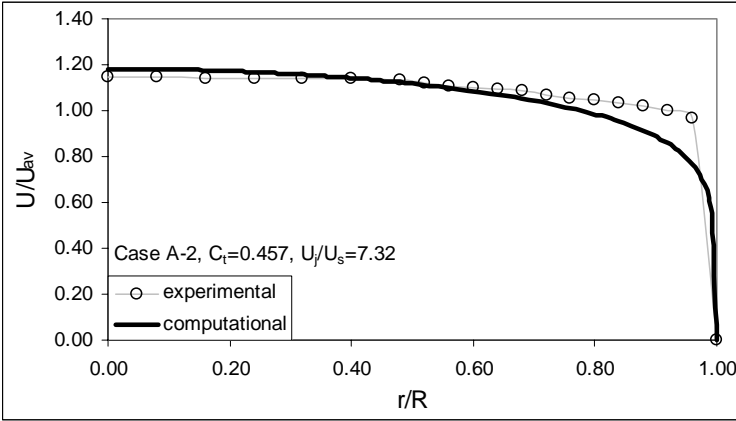


Figure 4.1: Dimensionless velocity profile for case A-2

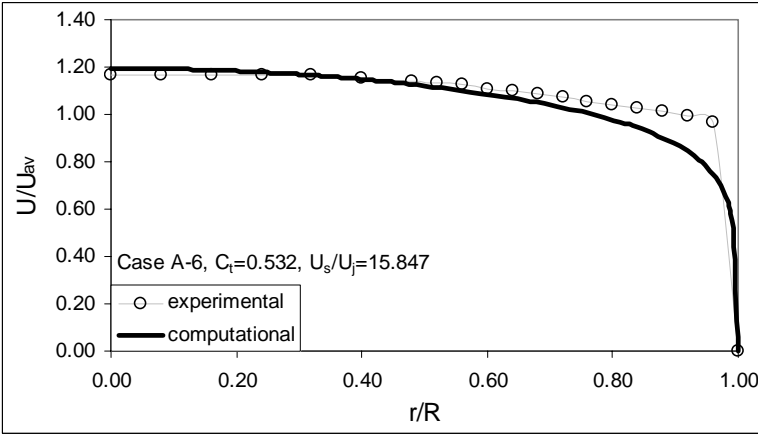


Figure 4.2: Dimensionless velocity profile for case A-6

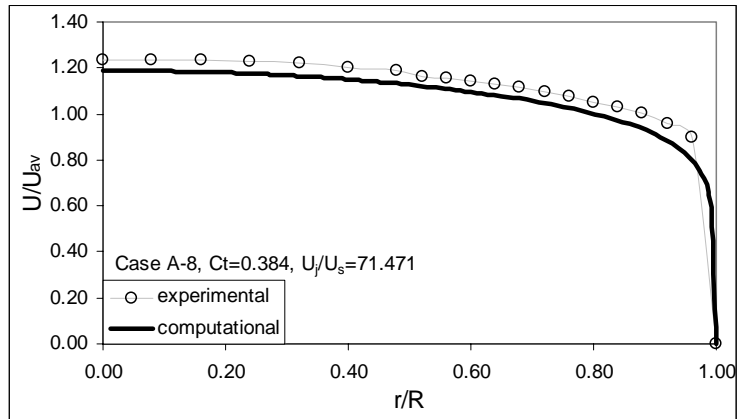


Figure 4.3: Dimensionless velocity profile for case A-8

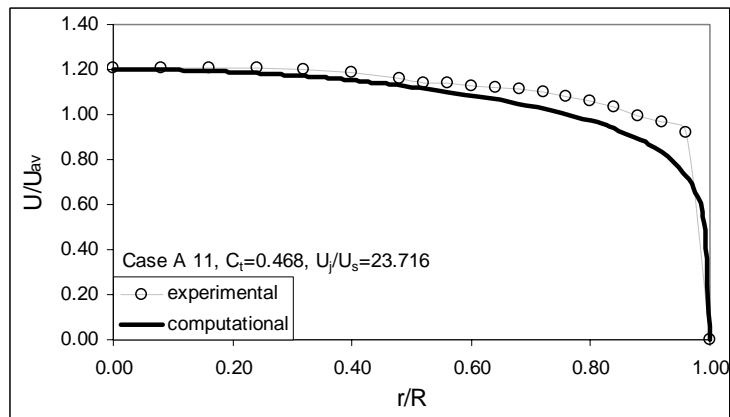


Figure 4.4: Dimensionless velocity profile for case A-11

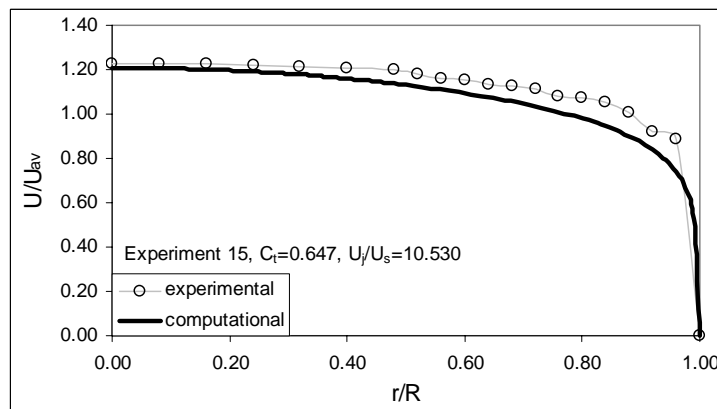


Figure 4.5: Dimensionless velocity profile for Case A-15

When the measured and computed velocity profiles are compared, near the wall of the pipe it is foreseen that there are differences in the velocity. One reason for this may be possible alignment changes of the jet pipe during the experiments. Other possibility is the miss alignment of the total head tube.

Velocity profiles across the mixing pipe are developed computationally for cases A-2, A-6, A-11 and A-15 having $Ct = 0.775, 0.532, 0.468,$ and 0.567 respectively and are shown in Figure 4.6. The local velocity profiles are nondimensionalized by computational average velocity for each case.

At the entrance undisturbed jet and secondary flow can be examined. Before mixing, these two flows are uniform pipe flow. Then, it is observed that jet flow entrains to secondary flow along a shear layer. Existing boundary layers and shear layers consumes the secondary flow. In cases 6 and 11, mean velocity has negative values due to separation of flow as a result of high kinetic energy of the jet. At the location of where $x / R = 84$ the flow recovers the uniform flow characteristic.

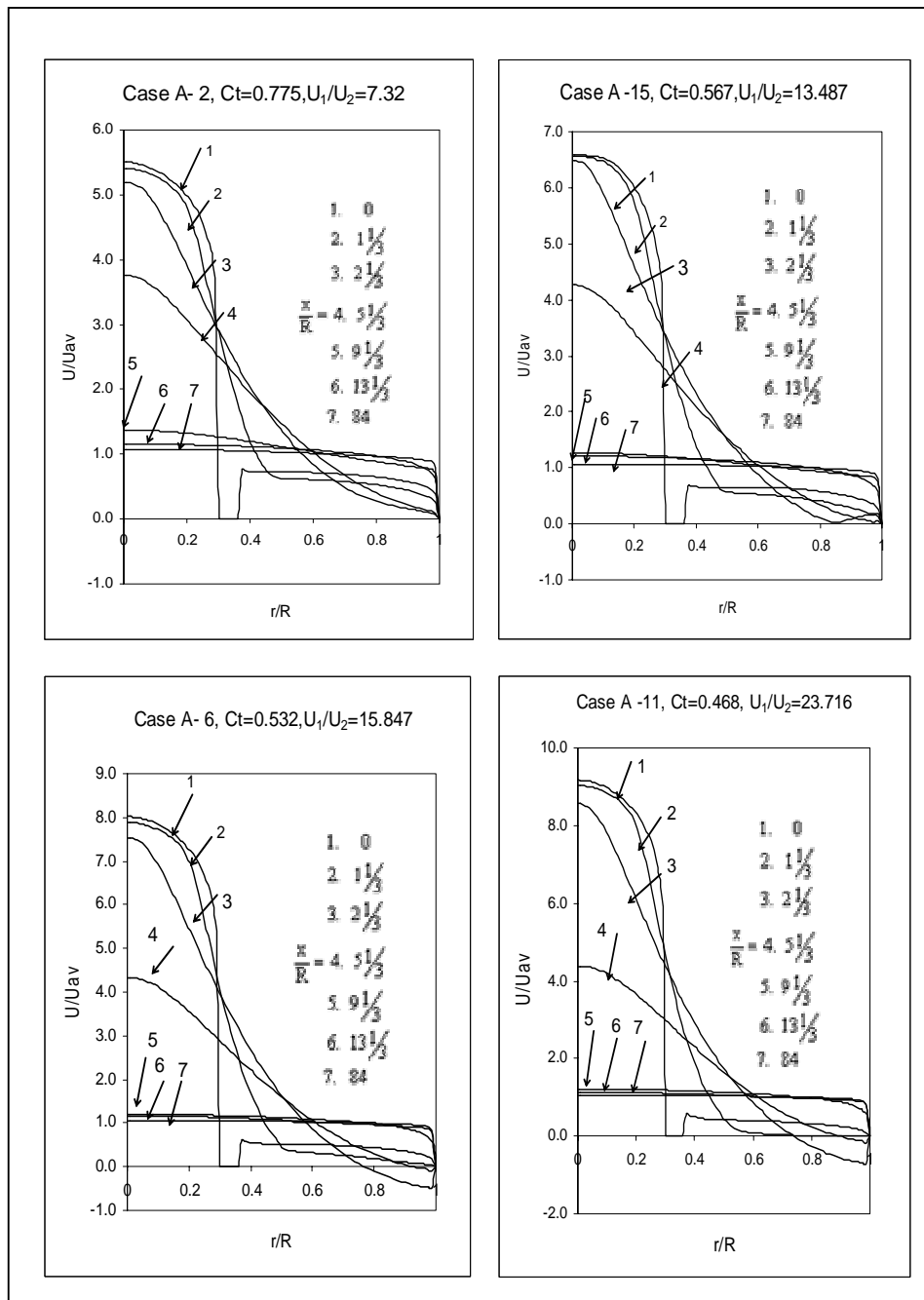


Figure 4.6: Mean velocities along the mixing pipe for cases A-2, A-6, A-11, and A-15

4.1.4. Experimental and Numerical Pressure Variation

In present experimental study, pressure variation along the mixing pipe wall is recorded. The pressure is defined relative to entrance wall pressure and nondimensionalized by dynamic pressure. The experimental and numerical pressure variations are shown in Figures 4.7 to 4.12.

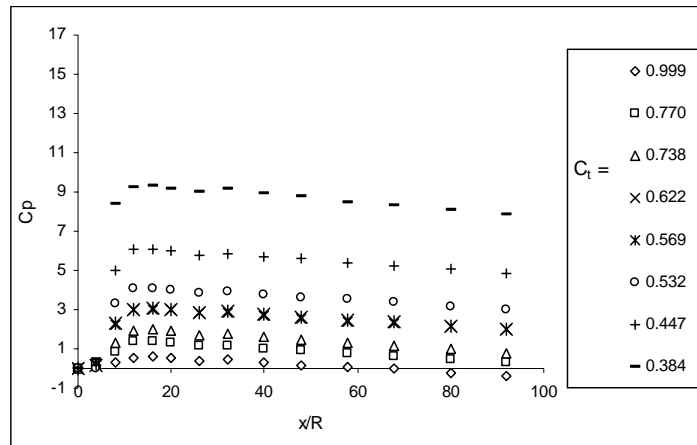


Figure 4.7: Experimental wall pressure variations for [A-1 and A-8]

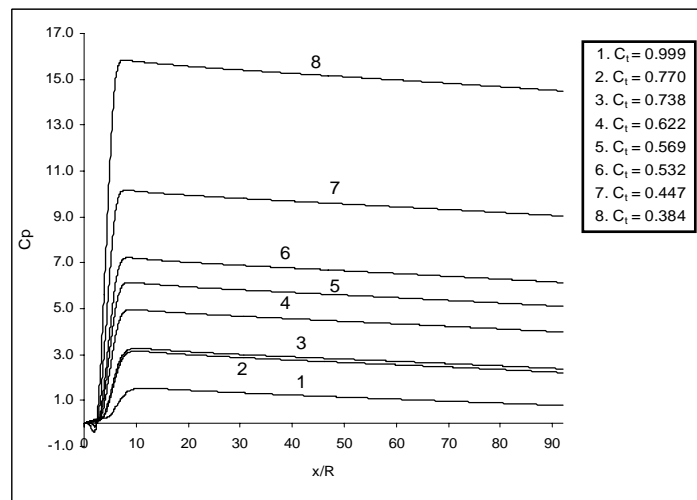


Figure 4.8: Computational wall pressure variations for [A-1 and A-8]

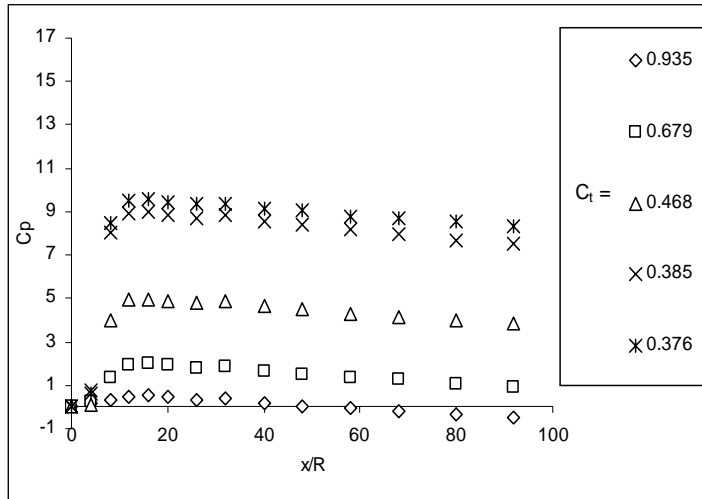


Figure 4.9: Experimental wall pressure variations for [A-9 and A-13]

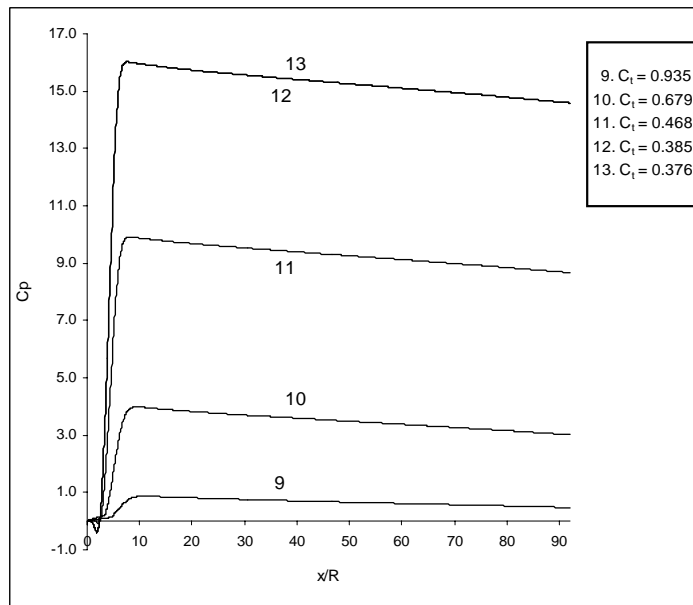


Figure 4.10: Computational wall pressure variations for [A-9 and A-13]

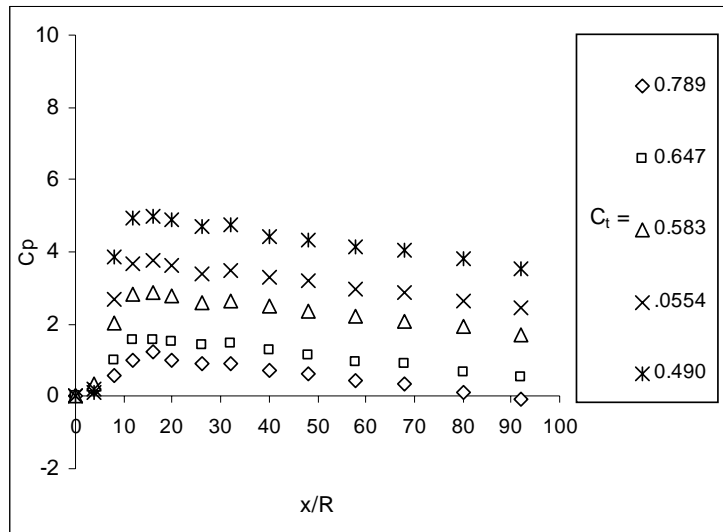


Figure 4.11: Experimental wall pressure variations [A-14 and A-18]

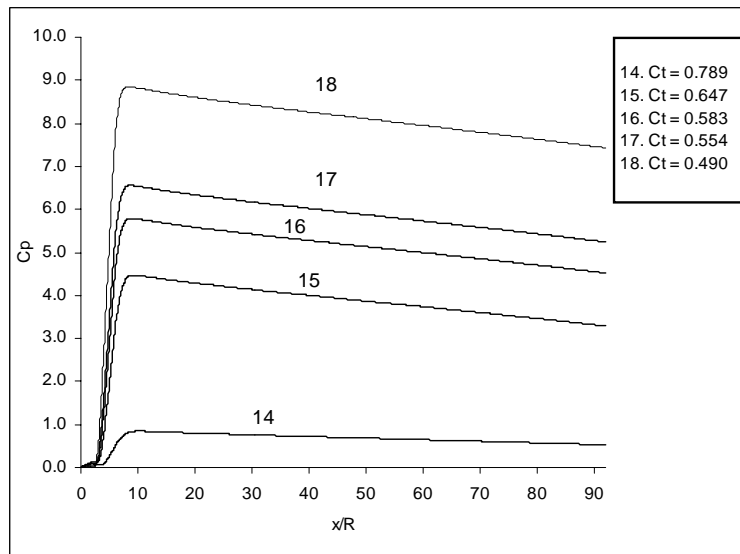


Figure 4.12: Computational wall pressure variations for [A-14 and A-18]

Observing the above set of pressure distributions, it is noticed that results of experimental and numerical analyses do not coincide with each other. Numerical results show higher results than the experimental ones. Different

sources of error may be the reason behind this discrepancy and they can be explained as follows.

To explain the reason of such error, the pressure distribution across the pipe is regenerated. In this analysis, the outflow pressure is set to zero and pressure across the pipe defined accordingly. In the experimental setup, there exist 5 piezometer tubes before mixing region. These piezometers are included while regenerating the pressure distribution. Therefore pressure distribution before and after mixing can be examined.

Experimental and computational pressure distributions across the pipe before and after the jet entrance are given in Figures 4.13 to 4.17 for cases A-2, A-15, A-6 A-11 and A-8. Examining these figures in both computational and experimental pressure have tendency to drop before the entrance. This is exactly consistent with uniform pipe flow. It is observed that overall pressure drop in the mixing region is smaller in measurements compared to numerically computed ones.

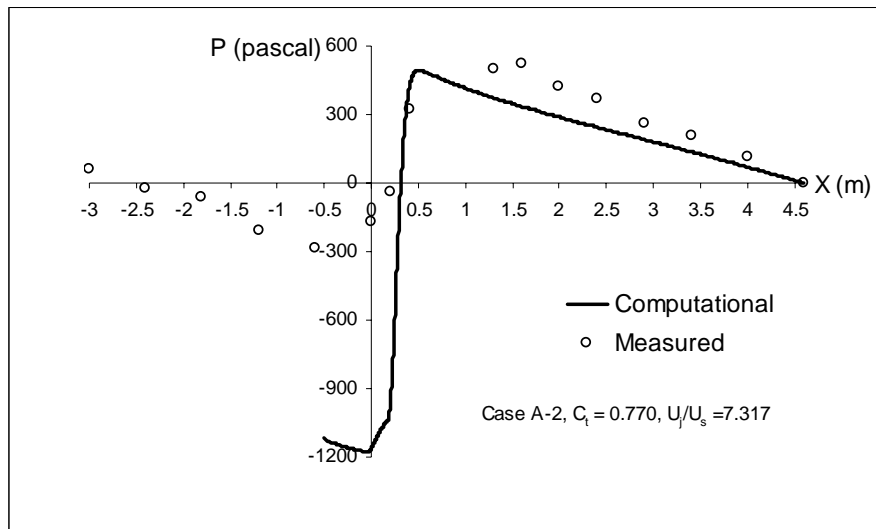


Figure 4.13: Pressure distributions across mixing pipe, Case A-2

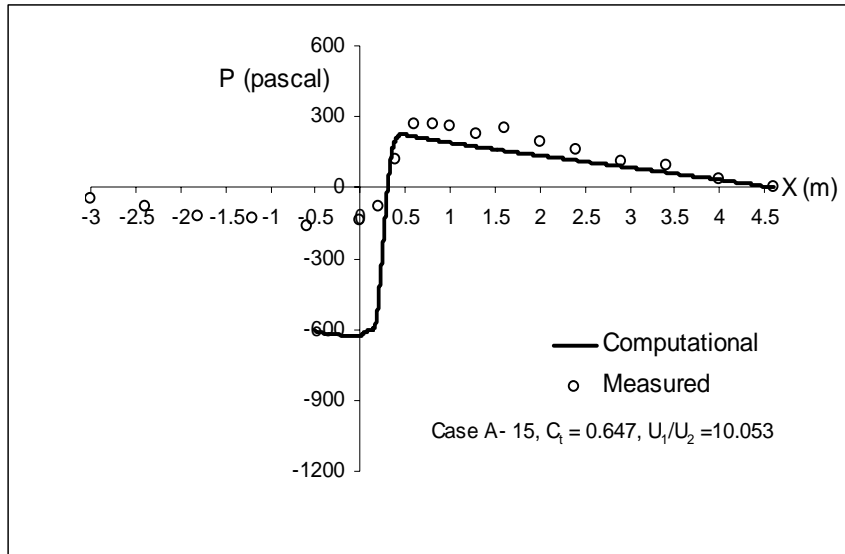


Figure 4.14: Pressure distributions across mixing pipe, Case A-15

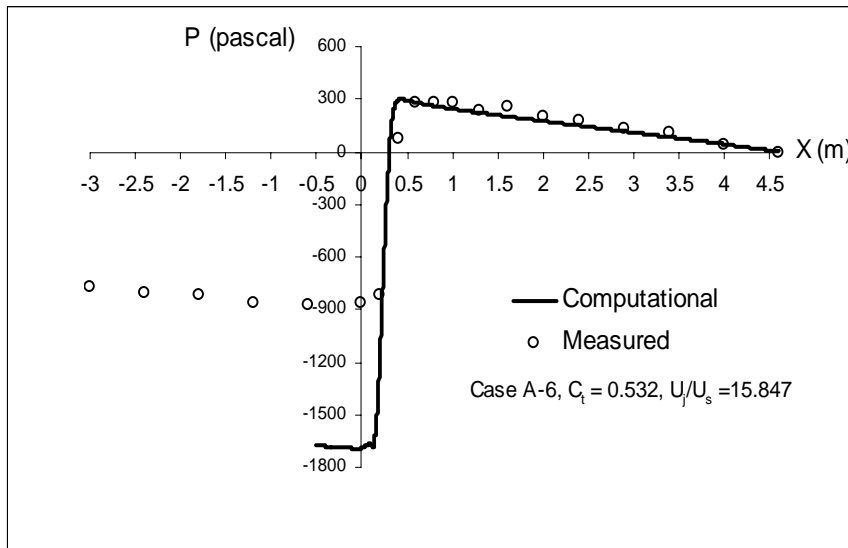


Figure 4.15: Pressure distributions across mixing pipe, Case A-6

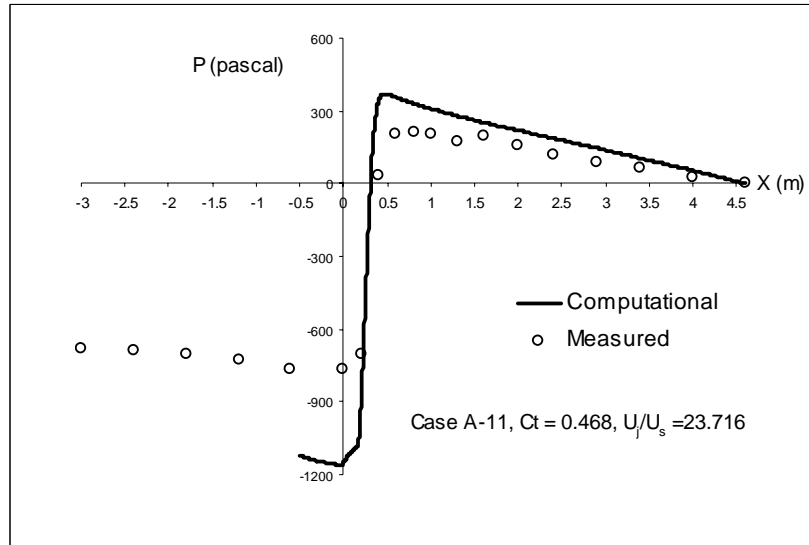


Figure 4.16: Pressure distributions across mixing pipe, Case A-11

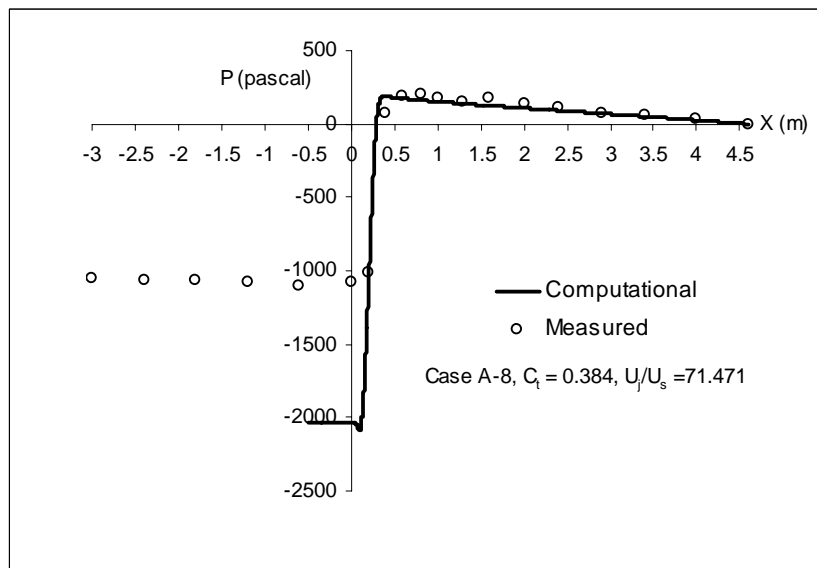


Figure 4.17: Pressure distributions across mixing pipe, Case A-8

The controlling parameter for confined coaxial jet is the Craya-Curtet number, which is in fact ratio of momentum in the mixing pipe after mixing to total momentum of primary and secondary flows. As a result flow conditions of

primary and secondary streams directly affect the pressure distribution in the mixing pipe so that initial flow conditions for primary and secondary streams must be determined accurately. In the present study, total discharge is calculated from weir and discharge of primary stream is estimated from pressure drop. Then the flow rate of secondary stream is computed by conservation of mass. In order to obtain same results in terms of pressure variation across the mixing pipe, numerical model should be developed with same initial conditions used in experiments. The discharges in the primary and secondary streams should be estimated separately by using flow rate measurement devices such as orifice meter. Flow in the duct also should be estimated, using an accurate measuring device or weir must be well calibrated. While running the experiments, the conservation of mass should be checked for each case.

4.2. RESULTS AND DISCUSSIONS FOR CASE B

In the study of the E. Razinsky and J.A.Brighton the properties of confined coaxial jets are explained in terms of pressure distribution, mean velocity distribution and turbulence characteristics.

Herein the condition summarized in Section 3.2 is modeled numerically and the imposed initial conditions are $U_j / U_s = 9$ and 5. In Figure 4.18 results of both computational and experimental studies are given. Under specified conditions, numerical studies show consistence with experimental studies.

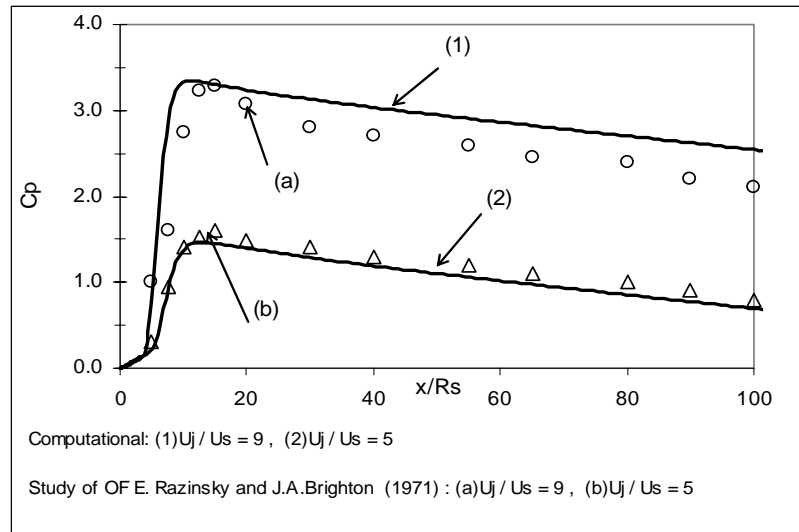


Figure 4.18: Wall pressure distributions ($R_j / R = 3$)

In addition to pressure distribution analyses also mean velocity profiles across the duct is defined numerically for velocity ratio of primary stream to secondary stream, $U_j / U_s = 9$ and radius ratio, $R_1 / R = 3$. In Figures 4.19 and 4.20 results of experimental study and corresponding computational results are given respectively.

In these figures it is observed that in the study of E. Razinsky and J.A.Brighton (1971), initial velocity profiles of the primary and secondary streams are treated as potential flow. In the numerical study these are considered as uniform flow therefore there are some inconsistencies between experimental results and computational results.

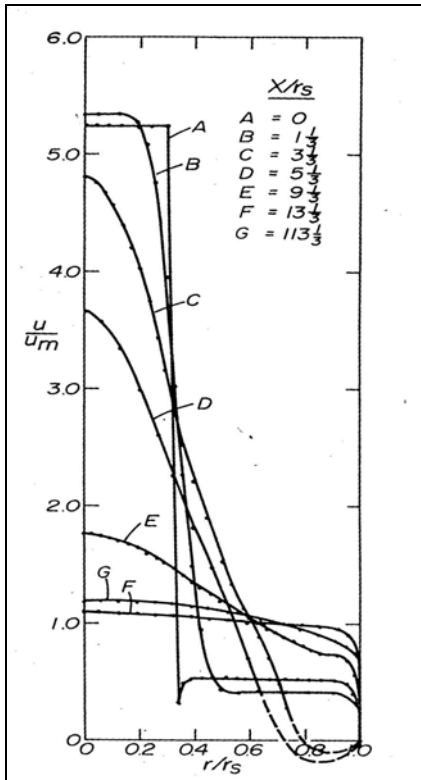


Figure 4.19: Mean velocity distribution across the duct (Study of Razinsky and Brighton (1971))

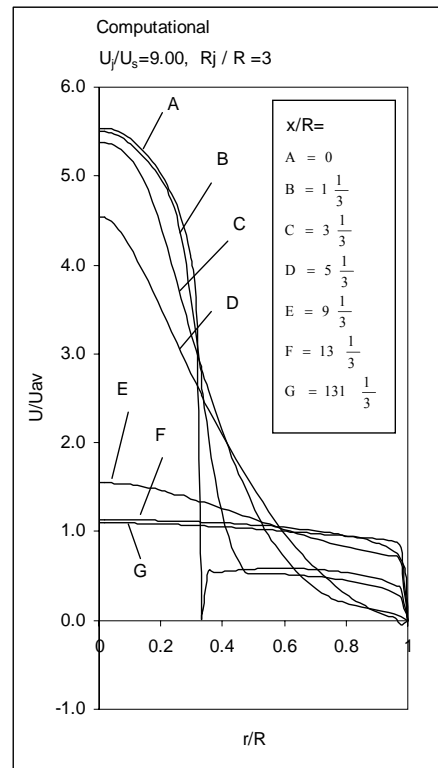


Figure 4.20: Mean velocity distribution across the Duct, Computational result.

4.3. RESULTS AND DISCUSSIONS FOR CASE C

After modeling the study of E. Razinsky and J.A.Brighton (1971) computationally, it is foreseen that if the initial conditions of primary and secondary streams are imposed correctly as they are defined in the experiments, the computational results well approach to experimental results. In this section, experimental study of Y. Shimizu, Y. Nakamura, S. Kuzuhara, S.Ktara (1987) will be modeled in order to observe this.

In this study, dimensionless pressure term is also denoted as C_p , however pressure is defined relative to suction pressure and relative pressures are nondimensionalized by dynamic head calculated from jet velocity so dimensionless pressure term is written as follows.

$$C_p = \frac{P - P_{so}}{\frac{1}{2} U_j^2 \rho} \quad [4.1]$$

The measured and computed pressure distributions in the mixing pipe for Cases C-1 and C-2 are given in Figures 4.21 and 4.22 respectively.

For Case C-3 the measured pressure distribution and computed pressure distributions are given in Figures 4.23 and 4.24.

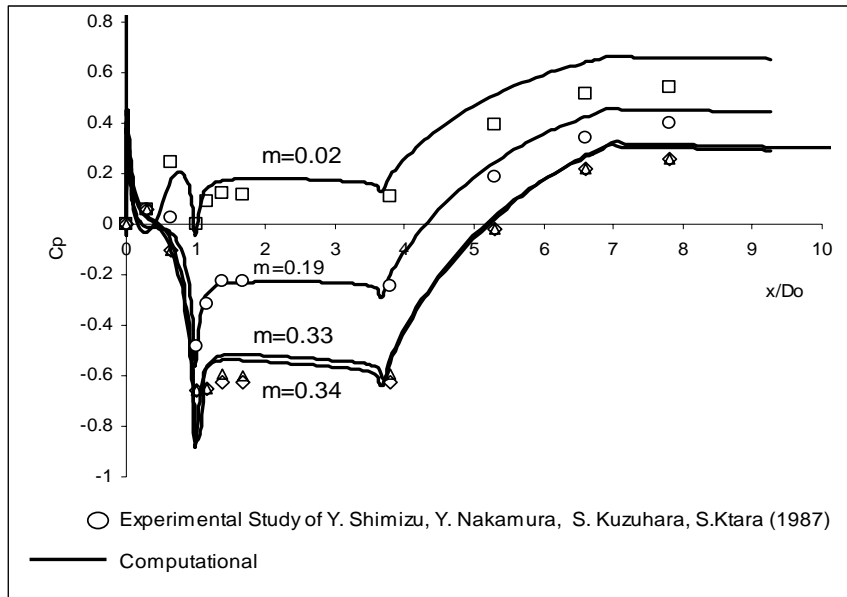


Figure 4.21: Experimental and computational results of study of Y. Shimizu, Y. Nakamura, S. Kuzuhara, S.Ktara (1987), Case C-1

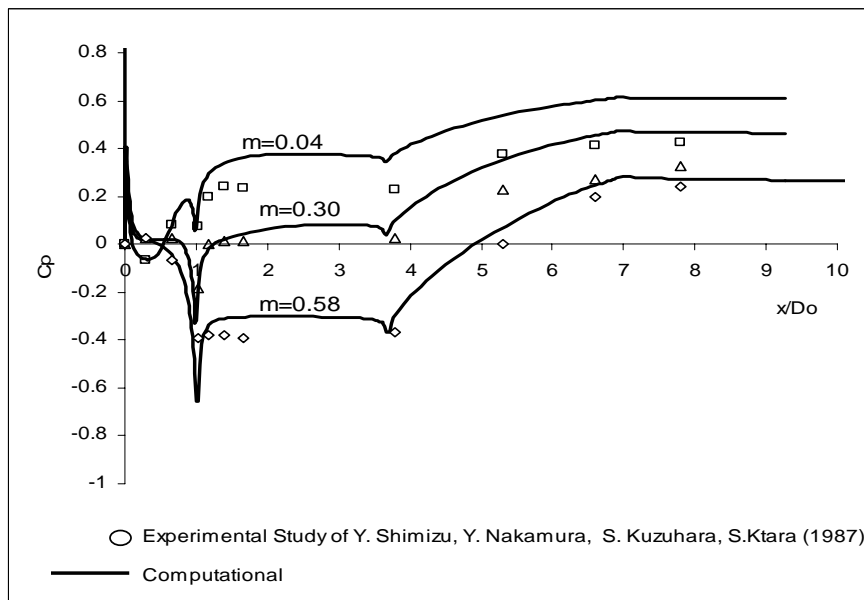


Figure 4.22: Experimental and computational results of study of Y. Shimizu, Y. Nakamura, S. Kuzuhara, S.Ktara (1987), Case C-2

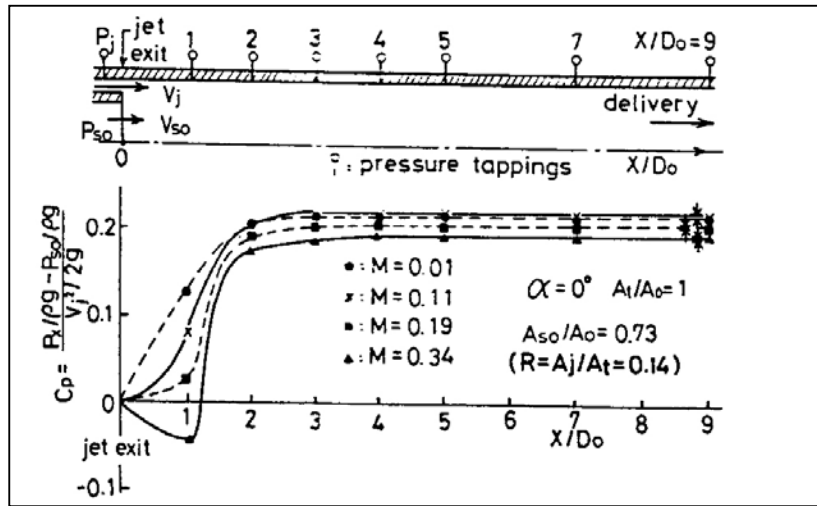


Figure 4.23: Experimental Results of Study of Y. Shimizu, Y. Nakamura, S. Kuzuhara, S.Ktara (1987), Case C-3

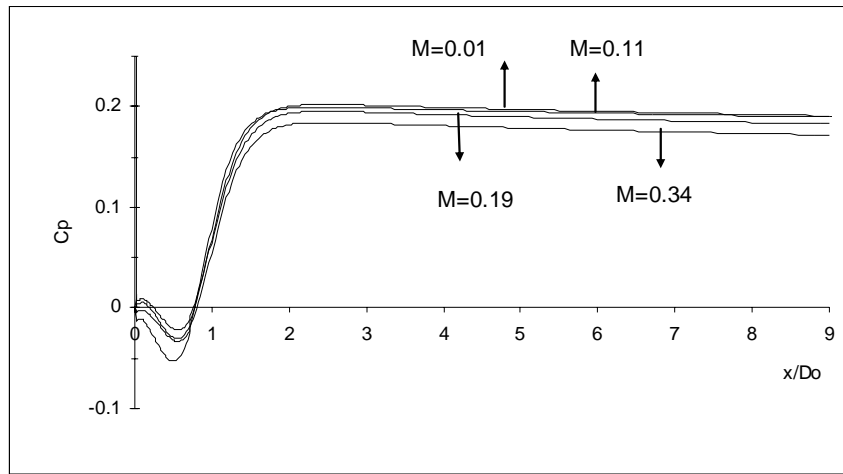


Figure 4.24: Computational results for study of Y. Shimizu, Y. Nakamura, S. Kuzuhara, S.Ktara (1987), Case C-3

4.4. SEPERATION BUBBLES AND ENERGY DISSIPATION

Accuracy of the numerical models is verified by previous studies. Therefore, present computational models can be used in further discussion in order to explain the flow properties of confined coaxial jet.

Observing the pressure variation along the pipe after mixing, it is justified that due to expansion of jet along the pipe, an adverse pressure gradient is developed. For strong jet flows having a larger primary velocity than secondary velocity, the adverse pressure develops rapidly comparing with the weak jets.

Herein the streamline velocities of several cases are given in order to explain the behaviors of confined coaxial flows. Considering the initial velocity ratio and corresponding Craya-Curtet number, the streamlines patterns of some selected cases are shown in Figure 4.25. The selected cases are as follows

Case A-2: $U_j / U_s = 7.317, C_t = 0.999$

Case A-15: $U_j / U_s = 10.053, C_t = 0.647$

Case A-11: $U_j / U_s = 23.716, C_t = 0.468$

Case A-8: $U_j / U_s = 71.471, C_t = 0.384$

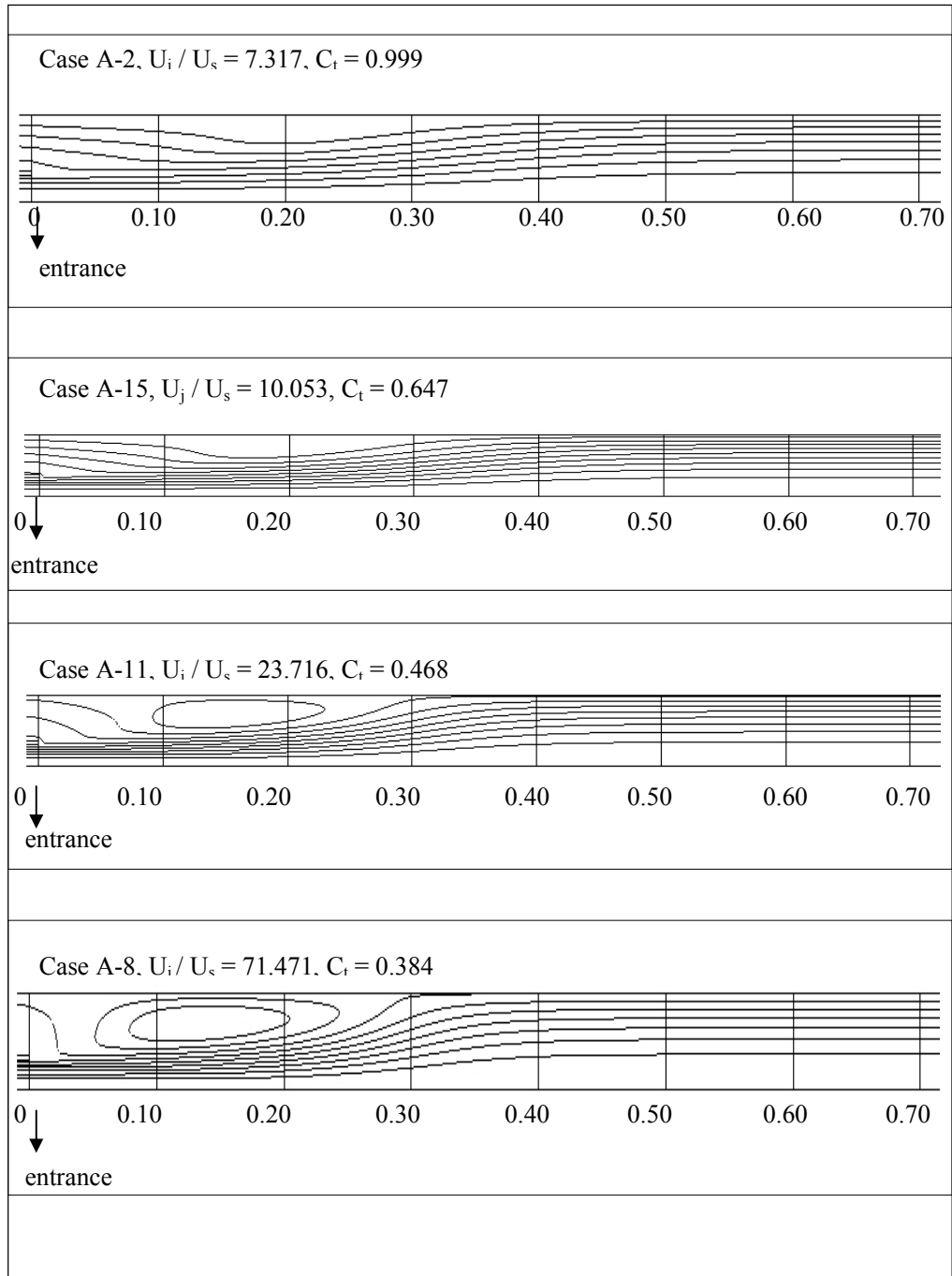


Figure 4.25: Streamline patterns for numerical solutions

These cases are sketched from lower velocity ratio to higher velocity ratio. In confined coaxial flow, when jet enters, two shear layer zones and boundary layer zones are developed. Jet expands in diameter along the shear zones. The secondary stream entrains inside the jet along the shear zone. Later secondary flow will be consumed by boundary and shear layers. If secondary flow is consumed before jet dissipates all of its energy, the jet expands to the pipe wall and separation of flow will take place.

For strong jets in which the jet velocity is well above higher than the secondary stream velocity, there exists high kinetic energy of flow. For case A-8, it is observed that secondary flow is exhausted very rapidly before jet loses its kinetic energy and system ends up with large eddies in the separation zone. The spreading rate of jet increases as the flow becomes turbulence and the turbulence increases the exchange of momentum. This property of turbulent is called as diffusivity. Due to kinetic energy of the flow, in high jets the large eddies will form rapidly and as a result high turbulence will be developed and this will dissipate energy and the momentum fast. In conclusion, mixing will be completed and uniform flow characteristics are recovered rapidly.

CHAPTER 5

CONCLUSIONS

Momentum exchange in coaxial jet flows is investigated experimentally. An experimental setup is constructed to estimate the momentum exchange rates and mixing of the two jet flows from the co-axial pipes. Pressure distributions along the outer pipe are measured for different flow ratios of the jets. In addition to present experiments, numerical data of two experimental cases from the literature are also considered as test cases. Numerical solutions for the test cases are obtained using FLUENT.

1. Measured pressure distributions for case-A and the corresponding computed values from FLUENT are not conforming on each other for the whole flow field. Computed pressure drop in the entrance region is higher than the measured values. This discrepancy is attributed to a possible error in experimental measurement of discharges from the weir or from the pressure drop in the pipes although it could not be verified.
2. Another possible source of error is inappropriate boundary conditions at the inlet section. It is difficult to verify existence of identical inlet conditions in the experimental and the numerical studies.
3. On the other hand, numerical results from FLUENT was encouraging when compared to experimental cases B and C. Better agreement was observed in pressure distributions.

4. Experiments may be repeated with more precise measurement of discharges, to present a conclusive comparison of experimental and numerical data.
5. An investigation of alternate turbulence models available in FLUENT may be conducted to improve the accuracy of numerical predictions.

REFERENCES

Mueller, N. H. G., "Water Jet Pump", Journal of Hydraulic Division Proceedings of the ASCE, Vol. 90, HY 3, 1964.

Reddy, Y.R. and Kar, S., "Theory and Performance of Water Jet Pump", Journal of Hydraulic Division Proceedings of the ASCE, Vol. 94, HY 5, 1968.

Sanger, N. L., "An Experimental Investigation of Several Low-Area-Ratio Water Jet Pumps" Transaction of the ASME, Journal of Basic Engineering, 1970.

Razinsky, E and Brighton, J. A., "Confined Jet mixing for Nonseparating Conditions", ASME Journal of basic Engineering, Vol. 93, no. 3, 1971.

Rajataman, N., Developments in Water Science 5 Turbulent Jets, Elsevier 1976.

Choi, D. W., Gessner F. B. and Oates, G.C., "Measurements of Confined Coaxial Jet Mixing with Pressure Gradient", Journal of Fluids Engineering, Vol. 108, 1986.

Shimizu, Y., Nakamura, S., Kuzuhara, and S., Kutara, S., "Studies of the Configuration and Performance of Annular Type Jet Pumps", Journals of Fluids Engineering, Vol. 109, 1987.

Khodadadi, J.M. and Vlachos, N. S., "Experimental and Numerical Study of Confined Coaxial turbulent Jets" AIAA Journal, Vol. 27, No. 5, 1989.

Elger, D.F., McLam, E. T., and Taylor, S.J., "A New Way to Represent Jet Pump Performance", Journal of Fluid Engineering, Vol. 113, 1991

Elger, D. F., Taylor, S. J., and Liou, C. H., “Measurements of Confined Coaxial Jet Mixing with Pressure Gradient”, *Journal of Fluids Engineering*, Vol. 116, 1994.